Science of the Total Environment 633 (2018) 1518–1535

Contents lists available at ScienceDirect

Science of the Total Environment

journal homepage: www.elsevier.com/locate/scitotenv

Potential impact of climate change on groundwater resources in the Central Huai Luang Basin, Northeast Thailand

Kewaree Pholkern [a,b], Phayom Saraphirom [a,c,*], Kriengsak Srisuk [a]

[a] Groundwater Resources Research Institute, Khon Kaen University, Thailand
[b] Department of Environmental Engineering, Faculty of Engineering, Khon Kaen University, Thailand
[c] Department of Agricultural Engineering, Faculty of Engineering, Khon Kaen University, Thailand

HIGHLIGHTS

- The central Huai Luang basin is underlain by rock salts resulting in spreading of groundwater and soil salinity.
- Climate change may impact on groundwater recharge, waterlogging and soil salinity distribution in this basin.
- Groundwater level, waterlogging and salinity distribution areas are projected to be increased, in the future precipitation.
- The soil salinity is the consequence effect that may exacerbate future livelihood conditions in this area.

GRAPHICAL ABSTRACT

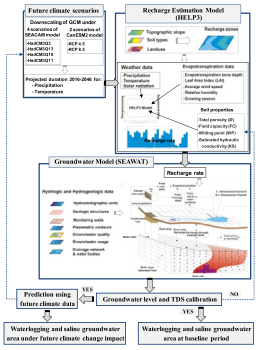

ARTICLE INFO

Article history:
Received 31 October 2017
Received in revised form 24 March 2018
Accepted 24 March 2018
Available online 4 April 2018

Keywords:
Climate change
Groundwater resources
Salinity
HELP3
SEAWAT
Huai Luang Basin

ABSTRACT

The Central Huai Luang Basin is one of the important rice producing areas of Udon Thani Province in Northeastern Thailand. The basin is underlain by the rock salt layers of the Maha Sarakham Formation and is the source of saline groundwater and soil salinity. The regional and local groundwater flow systems are the major mechanisms responsible for spreading saline groundwater and saline soils in this basin. Climate change may have an impact on groundwater recharge, on water table depth and the consequences of waterlogging, and on the distribution of soil salinity in this basin. Six future climate conditions from the SEACAM and CanESM2 models were downscaled to investigate the potential impact of future climate conditions on groundwater quantity and quality in this basin. The potential impact was investigated by using a set of numerical models, namely HELP3 and SEAWAT, to estimate the groundwater recharge and flow and the salt transport of groundwater simulation, respectively. The results revealed that within next 30 years (2045), the future average annual temperature is projected to increase by 3.1 °C and 2.2 °C under SEACAM and CanESM2 models, respectively, while the future precipitation is projected to decrease by 20.85% under SEACAM and increase by 18.35% under the CanESM2. Groundwater recharge is projected to increase under the CanESM2 model and to slightly decrease under the SEACAM model. Moreover, for all future climate conditions, the depths of the groundwater water table are projected to continuously increase. The results showed the impact of climate change on salinity distribution for both the deep and shallow groundwater systems. The salinity distribution areas are projected to increase by about 8.08% and 56.92% in the deep and shallow groundwater systems, respectively. The waterlogging areas are also projected to expand by about 63.65% from the baseline period.

* Corresponding author at: Department of Agricultural Engineering, Faculty of Engineering, Khon Kaen University, Thailand.
E-mail address: payosa@kku.ac.th. (P. Saraphirom).

https://doi.org/10.1016/j.scitotenv.2018.03.300
0048-9697/

1. Introduction

Groundwater plays an important role in Thailand because it is a source of fresh water for human consumption, agriculture, and industries, especially during periods of drought. Serving as the water supply for approximately 35 million people in rural and urban areas, groundwater resources play a major role. In Northeastern Thailand, at least 80% of the groundwater wells have been drilled and developed in the consolidated aquifers (Srisuk and Nettasana, 2017), which are underlain with the rock salt of the Maha Sarakham Formation at depths of about 50–1000 m from the ground surface. This rock salt is the source of saline groundwater and saline soils in this area at >40% and 35%, respectively (DGR, 2000; Arunin, 1996). The Central Huai Luang Basin (CHLB) is spatially affected by the saline groundwater and saline soils along the Huai Luang Floodplain. The CHLB is an important area in terms of the following: (1) the socio-economic status of the second biggest province in Northeastern Thailand, and (2) the Gross Provincial Product, GPP (NSO, 2016) due to these facts: (a) the CHLB is covered by commercial areas, and b) it is the most important rice producing area of Udon Thani Province. Groundwater and soil salinity problems have interrupted activities and have required a supply of water in this area, such as water for irrigation and agricultural purposes, etc.

The major processes responsible for spreading saline groundwater, soil water and saline soils and sub-surface water are groundwater flow and evaporation of soil water (Srisuk, 1994). In addition, naturally occurring salt affected areas are caused by subsurface flow which is a primary source of salinity (Allan, 1994). As early as the 1980s, it was recognized that various human activities are responsible for the spreading of salinization or secondary sources of salinity (Arunin, 1984; Beresford et al., 2001). These human activities include deforestation, the construction of reservoirs in areas in which there is an occurrence of shallow saline groundwater, salt production, and irrigation (Arunin, 1989; Yuvaniyama, 2004). These activities are beginning to dramatically affect the natural environment and to reduce the viability of the agricultural sector (Arunin, 1984; Beresford et al., 2001).

Global climate change is defined as a climate situation in any area that has changed or differed over the past 30 years (HAII, 2016) and as a consequence, has had an impact on various sectors, including water resources in all the regions around the world. Like other regions and countries in the world, Thailand is also facing climate change and is experiencing the effects associated with it. Thailand is particularly vulnerable to drought and to flooding as evidenced by several extreme climatic events in the recent past (CHRR, 2005). As the result of heavy rainfall, Thailand faced a big flood for several months during 2011 (World Bank, 2011). A few years later, Thailand experienced one of the worst droughts in decades (ONEP, 2016). Even though scenarios for future events of climate change are still being debated, it is likely that Thailand will be affected in complex ways by the consequences of climate change (Naruchaikusol, 2016). According to the meteorological data records from 1955 to 2014, the trend in the average annual temperature in Thailand was an additional increase in the number of warm days and nights (Chatdarong, 2009; TRF, 2011; Limsakul et al., 2010). Yet, the total amount of rainfall did not change significantly. There have been regional diverging trends in rainfall volume in Central and Eastern Thailand where decreases in total rainfall have been observed. However, there have been increasing amounts of rainfall in the Northeastern and Gulf regions, as well as in Metropolitan Bangkok (Limsakul and Singhruck, 2016). There have been significant increases in rainfall in the dry season and decreases in the wet season, which includes a decrease in the number of rainy days and increase in the number of days with intense precipitation (Limsakul and Singhruck, 2016). The entire changing trend of rainfall has led to changes in rainfall patterns during the wet season (May – October), with longer dry spells in the middle of the rainy season and more intense precipitation (Jarupongsakul, 2011).

Several earlier studies developed and applied future climate change in Thailand for different purposes (Chinvanno et al., 2009; Manomaiphiboon et al., 2009; Santisirisomboon, 2009; TRF, 2011). These studies were based on the Special Report on Emission Scenarios (SRES) published by the Intergovernmental Panel on Climate Change (IPCC) Fourth Assessment Report (AR4) (IPCC, 2007). By utilizing the dynamic downscaled model, PRECIS (Providing Regional Climates for Impacts Studies) of the Hadley Centre Climate Model version 3 (HadCM3) boundary data (a subset of CMIP3), the Southeast Asia Climate Analyses & Modeling (SEACAM) regional climate modeling experiment has been used to assess the capacity for simulating the major features of the Southeast Asian climate and for capturing the broadest range of future projections for temperature, monsoon characteristics, and for precipitation. The results indicated that there will be an increasing trend in the average annual rainfall and temperature in the period from 2016 to 2056 (Chinvanno, 2014). According to the IPCC Fifth Assessment (AR5) (IPCC, 2013), the temperature is predicted to increase by 1.8 °C over the next 4 decades (2055), and the precipitation for the whole country is predicted to increase by approximately 5% within 40 years under the Representative Concentration Pathways (RCP) 8.5 scenario (HAII, 2016). The expected changes in the amounts and patterns of rainfall and temperature will lead to an alteration of groundwater resources (Zektser and Loaiciga, 1993) which can change the recharge rates, can influence the quality of the groundwater, and can alter groundwater flow patterns. In addition, the expected changes may affect waterlogging (the depth of water table can upward movement to soil surface and cause the accumulation of salt), as well as the spreading of saline water. This is especially true in Northeastern Thailand in which there are existing problems with groundwater and soil salinity.

From 1990 to 2010, there were approximately 198 peer-reviewed publications that focused directly on climate change and groundwater, but the potential impact of climate change on groundwater (Pratoomchai et al., 2014) and the future of groundwater in the context of global and regional climate changes remain largely unknown (Toews and Allen, 2009; Green et al., 2011; Kurylyk and MacQuarrie, 2013). In Northeastern Thailand, changes in climatic variables can significantly alter the hydrologic cycle and groundwater recharge, both of which control the distribution of salinity within the shallow aquifer systems and thus, affect the availability of land for agriculture (Saraphirom et al., 2013a). Ghassemi et al. (1995) reported that this phenomenon has created an expansion of land salinity as shown by Casas and Pitaluga (1990) who investigated climatic changes expressed in Pampa Arenosa, Argentina, after 1971, due to significantly increases in the average annual rainfall of approximately 200 mm per year.

Numerical modeling is a quick and useful approach to assess the past and future groundwater resources in response to climate change (Pratoomchai et al., 2014) specifically the temperature and precipitation changes to groundwater recharge (Moeck et al., 2016). Saraphirom et al. (2013b) studied the impact of climate change on the salinization processes in the Huai Khamrian Sub-watershed in Northeastern Thailand by using a variable density groundwater model named SEAWAT, which was supported with recharge estimates from the Hydrologic Evaluation of Landfill Performance (HELP) model. The results of the recharge rates at the end of the 21th century were predicted, and it was found that shallow saline groundwater areas will increase by approximately 14%. However, there are no studies that show the impact of climate change on groundwater resources in the CHLB which is of socio-economic importance to Udon Thani Province, especially under SRES and RCP scenarios.

The objectives of this study are as follows: 1) to characterize the hydrologic and hydrogeologic frameworks of the CHLB, 2) to simulate the processes of groundwater flow and salinity distribution, and 3) to predict the impact of future climate on groundwater flow and salinity distribution by applying numerical models. This study involved the field characterization of soils, the hydrologic and hydrogeologic conditions, and the application of the hydrological model. These processes were carried out in order to estimate the groundwater recharge. Using variable density of groundwater, the groundwater flow model was used to

calculate the water tables, flow patterns, and groundwater salinity. The results and findings will be useful to assist decision-makers and stakeholders in formulating the appropriate policies for water resource management in the CHLB.

2. The area of study

The CHLB is located in the central part of the Huai Luang Basin in Udon Thani Province in Northeastern Thailand. It covers an area of 1529 km^2 and is located in three districts of Udon Thani Province: Muang Udon Thani, Kut Chap, and Nong Wua So, as shown in Fig. 1. The topographic elevations vary from 160 to 564 m above Mean Sea Level (m AMSL). The mountainous and hilly terrains abound in the Western, Southern, and Northern regions which represent the surface water and groundwater divides of the basin. A population of about 448,000 persons or about 29% of Udon Thani Province's population are living in the basin (DPA, 2014). The Central Huai Luang Basin is one of the important agricultural and food production areas in Udon Thani Province. This area is underlain with rock salt from the Maha Sarakham formation, and this causes the spread of salts into the groundwater, the surface water, and the soil.

The area of study has a tropical grassland climate or Savanna-Aw in which the average daily temperature is 27.0 °C. January is the coolest month with a daily temperature of about 22.4 °C and approximately 29.8 °C in April which is the hottest month (TMD, 2015). An average evaporation from the Class A Pan measurement is 1683 mm/year (TMD, 2015). The average annual rainfall was calculated from the Udon Thani meteorological station using 11 rain gauge stations (TMD, 2015; RID, 2015) between 1984 and 2015. Almost 90% of rainfall occurs in the rainy season from May through October. The average annual rainfall varies from 1100 to 1500 mm (Average = 1268.6 mm).

The hydrological and hydrogeological study of the area were systematically characterized and presented as hydrogeologic maps and cross-sections. The procedures of drilling pumping test wells, installing piezometers (33 wells), monitoring the water levels, checking the quality of the groundwater and surface water, analyzing the soil moisture, and testing for soil salinity were all conducted during the period from September 2014 to December 2015. The Huai Luang reservoir in located in the Southwest and the Huai Luang River is a major water source of water and the supply for irrigation. The Huai Luang River flows from the west to the east with a length, width, and a depth of 50 km, 50–90 m, and 5–7 m, respectively. Along the Huai Luang River, two stream gauging stations are located at Kh.53 and Kh.103 (RID, 2015).

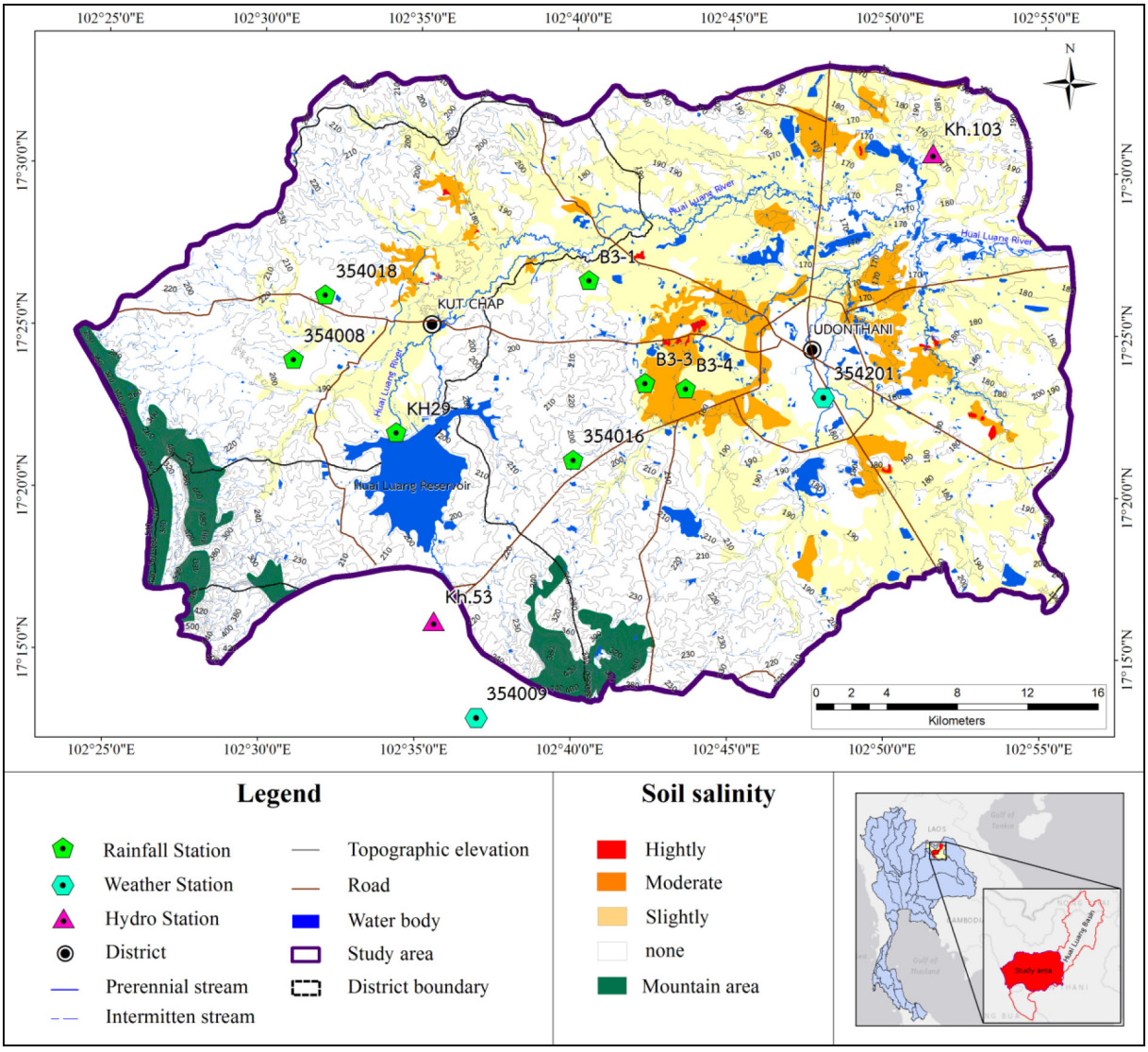

Fig. 1. Location map of the CHLB and soil salinity distribution.
(Modified from LDD, 2006)

The total annual runoff for the CHLB is around 262.4 MCM/year (Mm^3/year). The surface water salinity was monitored by measuring the electrical conductivity (EC) across the basin. During the dry season, the water quality of the Huai Luang River and its tributary are mildly brackish with electrical conductivities of >1500 μS/cm or Total Dissolved Solids (TDS) of >1000 mg/l, whereas during the rainy season, the surface water becomes slightly brackish to fresh.

Based on the saturated hydraulic conductivity values, soil are classified into three groups: slow, moderate, and rapid (Farr and Henderson, 1986). The slow soils have very slow infiltration rates ($<5 \times 10^{-7}$ m/s) and consist chiefly of clay soils. In the lowlands along the Huai Luang River, silty clay soil occurs over a nearly impervious material. The moderate soils have infiltration rates (5×10^{-7} to 5×10^{-6} m/s) and consist of moderately well-drained soils as fine to moderately fine textures, such as loam and sandy clay loam. These soils are mostly located in upland areas. The rapid soils have high infiltration rates ($>5 \times 10^{-6}$ m/s) and consist of excessively well-drained materials, such as loamy sand and sand. Most of the area is covered with moderately infiltrated soils and covers about 52% of the land area. The soil salinity in the area typically commences with deforestation in the recharge area, salt making, and the replacement of the trees with shallow root crops in the lowlands or local discharge areas. These practices have significantly led to a rise in the water table, to a rise in the recharge rates in the local recharge areas, and to the escalation of salinity problems (Arunin, 1984; Srisuk, 1994). The soil salinity was classified based on salt crust occurring on ground surface and giving rise to saline soil. As shown in Fig. 1, the soils were affected by salt at about 35%. Highly salt-affected soil covered about 0.1% of the studied lowland area, and the saturation extract (ECe) had an electrical conductivity of >8 dS/m. Moderately saline soil covered the lowland of the central and eastern parts of the studied area with ECe about 4–8 dS/m. Slightly saline soil was found upland in the western and southern parts of the studied area with ECe about 2–4 dS/m. In highly salt-affected areas, crops cannot be grown. Most of the area had been abandoned and invaded by salt tolerant weeds. In contrast, farmers in the slightly and moderately salt-affected areas can grow rice, but the plant growth is not uniform (Wichaidit, 1997). A rough approximation of decrease in the rice yield, caused by salinity of moderately saline soil, is >50% in susceptible cultivars, while the reduction of rice production in the slightly saline soil is only about 10–50% (Dobermann and Fairhurst, 2000). The land usage types are mainly paddy fields, field crops (sugarcane and cassava), urban areas, bodies of water, and forests. The paddy fields, which are located along Huai Luang River floodplain and in the eastern parts, occupied about 40% of the land. There is only one crop of rice that grows each year from May to November in the rain-fed agricultural area, whereas in irrigated areas, crops can be grown twice per year. Field crops are grown in the northwestern to southwestern regions and cover about 23% of the total land area, while forested areas, urban areas, and water bodies cover 19%, 13%, and 5%, respectively (LDD, 2013).

The comprehensive hydrogeologic map and some cross-sections across the studied area were reconstructed by using the field investigations and the existing data that had been compiled from the previous works (DMR, 2009; Suwanich, 1986; Cotanont, 2014) as shown in Fig. 2. The flood plain of the Huai Luang River is covered with sand, clay, and gravel of Alluvium (Al). In addition, Terrace (Te) Deposits are found in the hilly areas in the southern region. These unconsolidated units, having an average thickness of 30 m, are underlain by siltstone and sandstone aquifers of the Upper Phu Thok (Upt) unit. The Lower Phu Tok (Lpt) unit consists of shale and mudstone with a thickness of 50 to 200 m which is underlain by the rock salt layers of the Maha Sarakham (Ms) unit. The Khok Kruat (Kk) unit is found at the toe of the mountain and consists of siltstone and sandstone with a thickness of 430 to 700 m. The Lower Khorat Group (Lkg) Unit lies underneath the Kk unit and consists of sandstone, siltstone, claystone, and conglomerate. According to water level measurements from 2014 to 2015, the groundwater flow nets have been conceptually constructed in Fig. 2 and present the regional and local groundwater flow patterns. Generally, in the recharge areas, groundwater recharges to aquifers are located in the West, South, and the local high areas in the North. In contrast, the discharge areas are normally located along central part of studied area and the Huai Luang River floodplain. Throughout the basin, the Total Dissolved Solids (TDS) of the groundwater varies from <1000 mg/l (fresh) to <10,000 mg/l (brackish) and to >10,000 mg/l (saline). The high TDS or salinity varies with the depth of the water and is found in the lowland areas at the central part of studied area along Huai Luang River. Groundwater types vary from recharge areas to discharge areas and include Ca-HCO_3, Ca-Na-HCO_3 and Na-Cl, Na-Cl types (Deutsch, 1997).

There are about 650 water wells being used for domestic, agricultural, and industrial purposes. Most of the domestic wells were provided by the Department of Groundwater Resources. Water wells were drilled at depths ranging from about 20 to 122 m below the ground surface. According to the field survey and the census of water use in 2015, it was found that groundwater resource was being used for domestic, agricultural, and industrial purposes at ratio of 75%, 20%, and 5%, respectively. The total annual groundwater usage within the basin has been estimated at about 6,758,606 m^3, which is a relatively small volume when compared to the activities and the population in the studied area. This was due to the fact that some communities are located in areas with saline groundwater. As a result, it was necessary for alternative sources of water supply to be allocated by the Provincial Waterworks Authority (PWA).

3. Methodology

This work is underpinned by the need to thoroughly understand the hydrogeologic systems and the salinization processes. The structural diagram of the methodology and the required data are illustrated in Fig. 3. The saline water transport, water budgets, and waterlogging were simulated by using the variable density groundwater model (SEAWAT version 4 groundwater flow): saline water transport, water budgets, and waterlogging (Langevin et al., 2008). Recharge rates were estimated based on the HELP3 Model (Schroeder et al., 1994) and climate variables such as temperature and precipitation. After certain calibrations had been completed for both the SEAWAT and HELP3 models, simulations of groundwater flow and salt transport were conducted under the future climate variables from 2 sets. In the first set, the GCMs (General Circulation Models) were retrieved from the CMIP3 (Coupled Model Intercomparison Project 3) data portal under 4 scenarios of SEACAM. In the second set, the GCMs were retrieved from the CMIP5 data portal under two scenarios of CanESM2 as discussed in Section 3.2. These simulations were accomplished in order to examine the impact of climate change on groundwater resources with respect to both quantity and quality. The projected climate scenarios were used as the input data for the net recharge estimations. Groundwater levels, flows, salinity distribution patterns, and water table depths in the uppermost layer of the model were all used to assess the degrees of shallow groundwater salinization and distribution. The impact of future climate change on waterlogging and salinity distribution was evaluated by using the means of the areal distribution of the water table depths and by expanding the boundaries of the saline groundwater, which were taken from simulation results projected over the coming 30 years (2016 to 2045) for each climate scenario.

3.1. Numerical model

In this study, the physically-based hydrologic models, USGS SEAWAT Version 4 (Langevin et al., 2008) and HELP version 3.07 (HELP) (Schroeder et al., 1994), were used to estimate changes in the recharge rate, water balance, and salinity distribution in the CHLB.

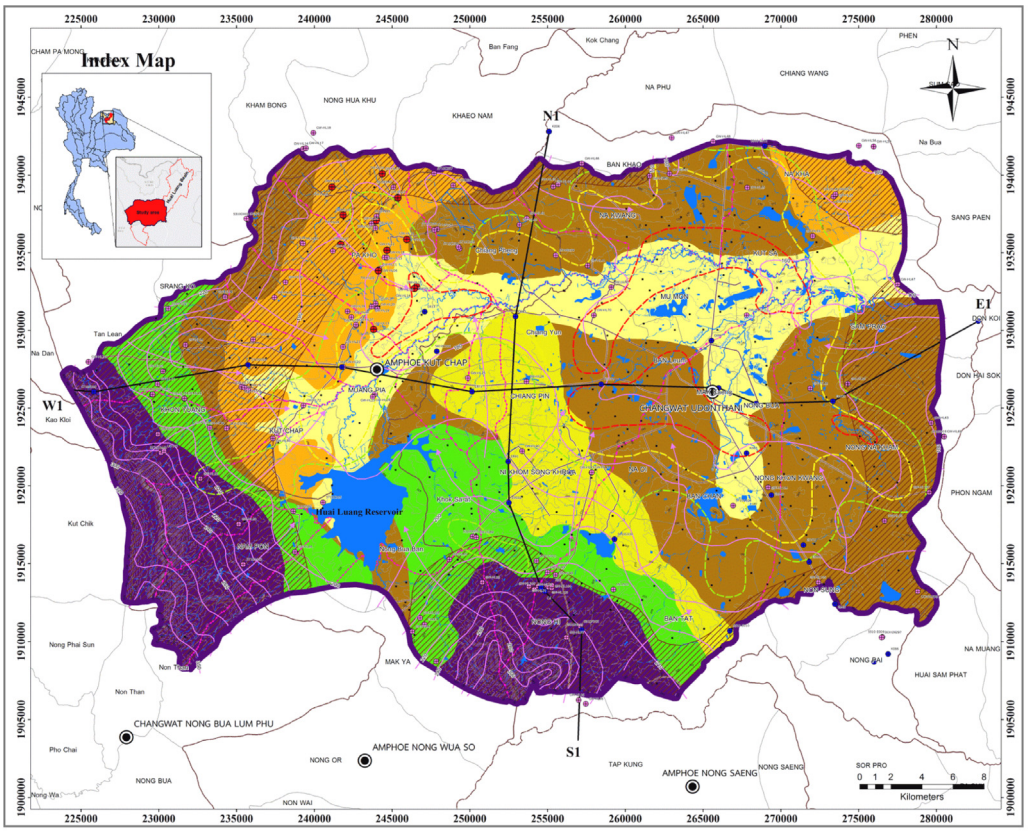

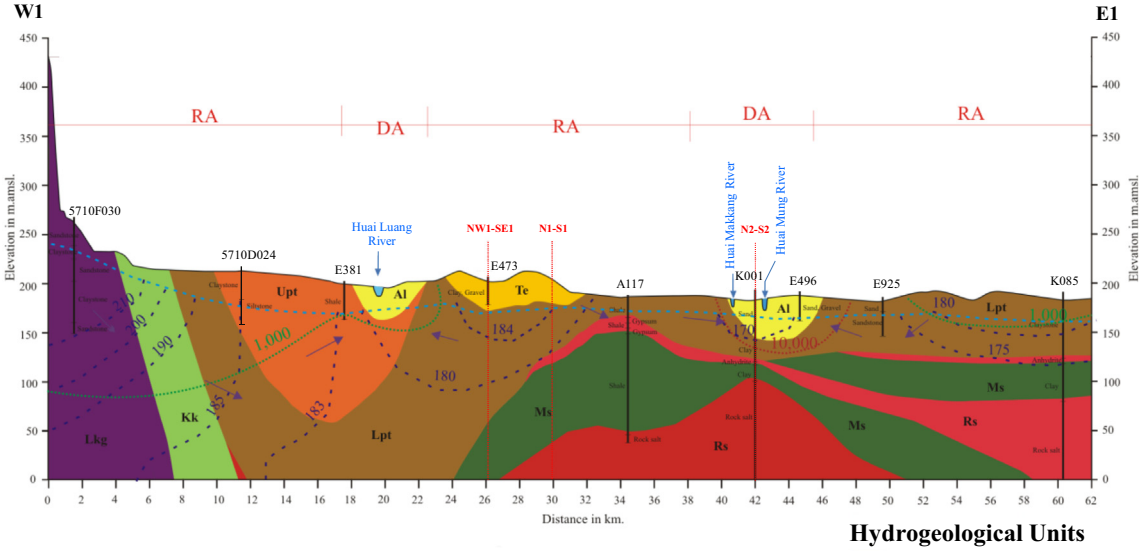

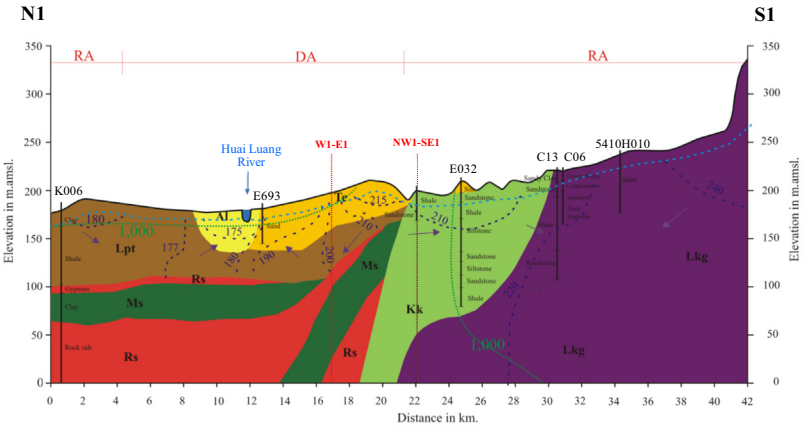

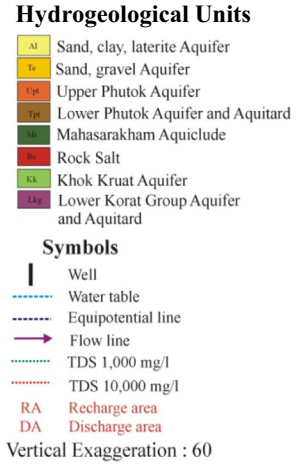

Fig. 2. Hydrogeologic maps and cross-sections of the CHLB.

3.1.1. Groundwater flow and salt transport

The SEAWAT program is a coupled version of MODFLOW (Harbaugh et al., 2000) for groundwater flow and MT3DMS (Zheng and Wang, 1999) for advective-dispersive transport. Together, SEAWAT is designed to simulate three-dimensional variable density saturated groundwater flows. Flexible equations were added to the program to allow the fluid density to be calculated as a function of one or more MT3DMS species. Fluid density may also be calculated as a function of fluid pressure. The effects of the fluid viscosity variations on groundwater flow were included as an option. Fluid viscosity can be calculated as a function of one or more MT3DMS species, and the program includes additional functions that represent the dependence upon temperature. Having the ability to combine flexible equations for fluid density and viscosity with multi-species transport, the SEAWAT Version 4 allows for variable-density groundwater flow coupled with multi-species solute and heat transport (Langevin et al., 2008). The Variable-Density Flow (VDF) Process in SEAWAT solves the following form of the variable-density ground-water flow equation (tensors and vectors are shown in bold.):

$$\nabla \cdot \left[\rho \frac{\mu_0}{\mu} \boldsymbol{K}_0 \left(\nabla h_0 + \frac{\rho - \rho_0}{\rho_0} \nabla z\right)\right] = \rho S_{s,0} \frac{\partial h_0}{\partial t} + \theta \frac{\partial \rho}{\partial C} \frac{\partial C}{\partial t} - \rho_s q'_s \quad (1)$$

ρ_0 is the fluid density [ML^{-3}] at the reference concentration and reference temperature; μ is the dynamic viscosity [$ML^{-1}T^{-1}$]; $\boldsymbol{K}_0$ is the hydraulic conductivity tensor of material saturated with the reference fluid [LT^{-1}]; and h_0 is the hydraulic head [L] which is measured in terms of the reference fluid at a specified concentration and temperature (as the reference fluid is commonly freshwater). Furthermore, $S_{s,0}$ is the specific storage [L^{-1}], which is defined as the volume of water that is released from storage per unit volume per unit decline of h_0; t is time [T]; θ is porosity [−]; C is salt concentration [ML^{-3}]; q'_s is a source or sink [T^{-1}] of fluid with density ρ_s; and z is the elevation head [L].

The limitations of SEAWAT Version 4 do not explicitly allow for the dissolution and precipitation of minerals that may likely result from

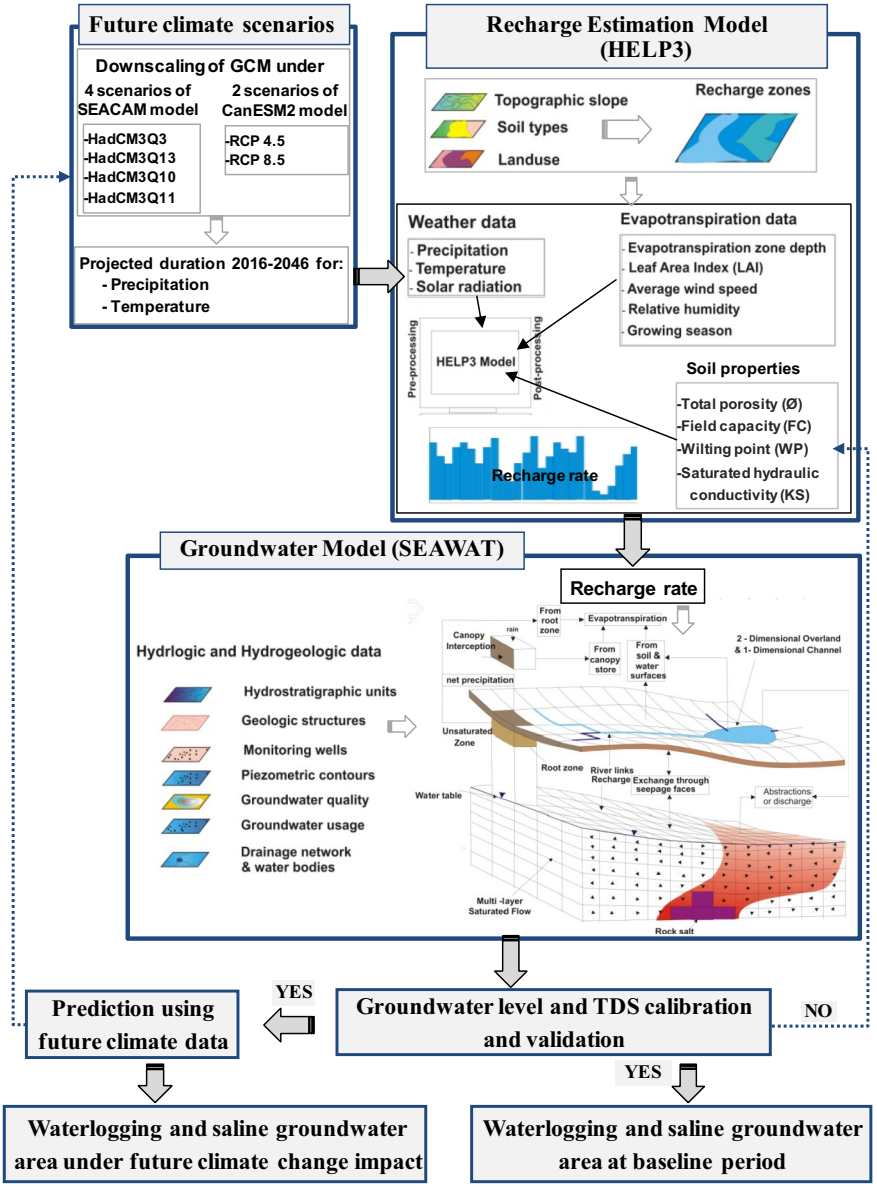

Fig. 3. Structural diagram of the modeling approach and required data.
(Modified from Saraphirom et al., 2013b)

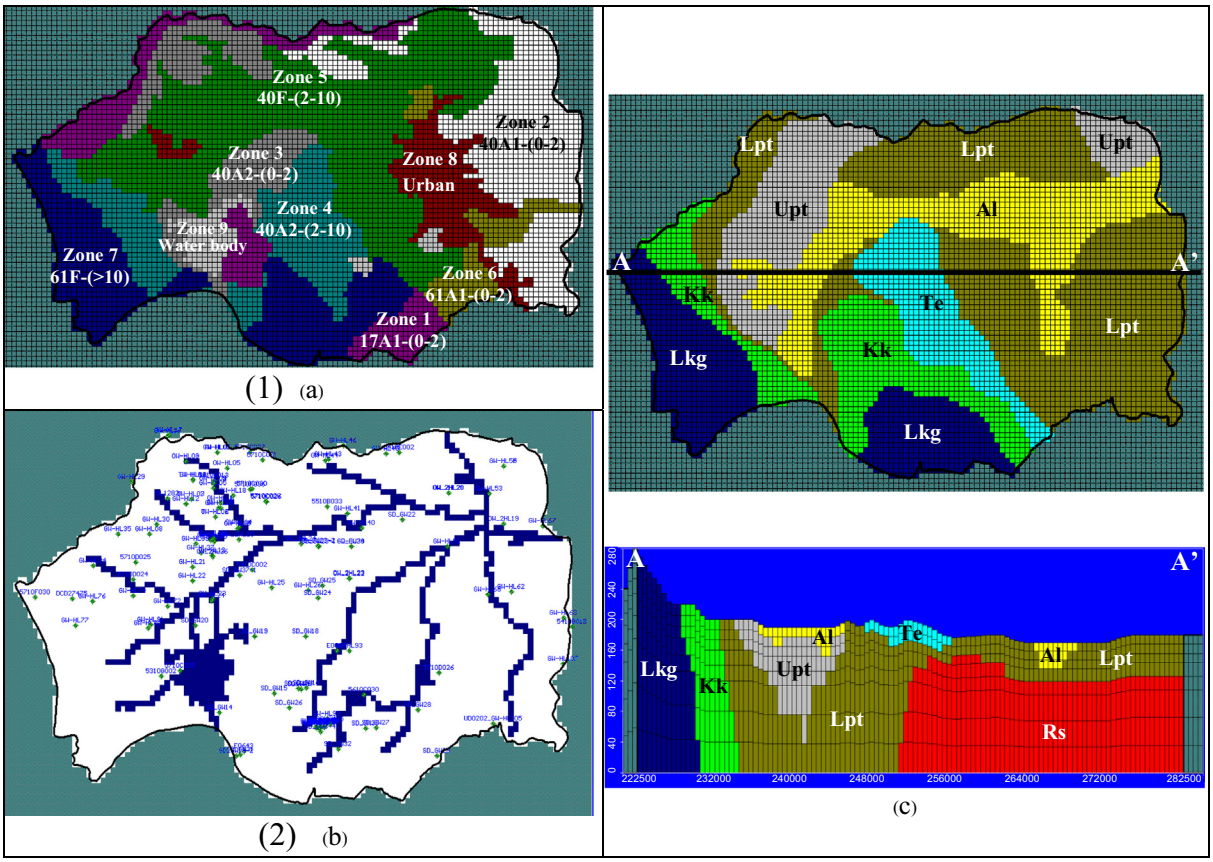

Fig. 4. Recharge zones (a), River boundary and Observation wells (b), and Grid design and distribution of the Hydraulic parameters (c) of CHLB model.

large temperature changes and the heat which is lost or gained from those reactions. The formulation is represented for water in the liquid phase only and does not represent the transitions to ice or to vapor.

SEAWAT model was selected to simulate groundwater flow and salt transport. The groundwater model domain has been identified by the physical boundaries of the CHLB (Fig. 4). Seven hydrostratigraphic units (aquifers and aquitards) have been assigned to the model as follows: (a) the sand, clay, and gravel of the Al and the Te units with a thickness of 10–30 m, (b) the siltstone and the sandstone aquifers of the Upt unit with thicknesses of 30–200 m, (c) the siltstone and sandstone aquifers of the Kk unit and Lkg unit with a thickness of 430 to 700 m, and (d) the claystone of the Lpt unit which is underlain by the rock salt layers of the Ms unit. This Ms unit was treated as a no flow boundary. The lateral boundaries and the bottom boundary of the flow domain were treated as no flow. The volume of General Head boundaries (GHB), assigned for Huai Luang River where the studied area was cut off from the whole basin, were collected from hydrological station Kh.103. The groundwater recharge was calculated using HELP3 model as discussed in Section 3.1.2. The drainage system and river input parameters including the river stage and width, and the vertical hydraulic conductivity, were measured during the field investigations and experiments.

The model was designed as a finite difference grid with a spatial resolution of 500 m × 500 m. The model was separated into 8 layers ranging from 10 to 40 m in thickness, between the altitudes of the topography to the lowest layer of mean sea level (AMSL). The upper layers (Layer 1- Layer 3) were assigned with a thickness of 10 m. The ranges of the input parameters were values of the following: vertical and horizontal hydraulic conductivity; specific yield and storage; total and effective porosity; and dispersivity. The model was calibrated and validated using some previous groundwater levels and salinity monitoring from Cotanont (2014) and information from the current study, such as pumping tests, dispersivity tests, groundwater levels, and salinity monitoring. The pumping test and dispersivity test results for each hydrogeologic unit are shown in Table 1. The initial conditions of the hydraulic heads and groundwater salinity were assigned from measurements taken in September of 2014 on the 152 observed wells. A constant concentration of 100,000 mg/l of saline water was assigned to represent the rock salt layer. The seasonal groundwater abstraction from each aquifer layer was obtained from the investigation during

Table 1
Flow and mass transport parameters used in SEAWAT model.

Hydrogeologic units	Horizontal hydraulic conductivity, Kh (m/s)	Vertical hydraulic conductivity, Kv (m/s)	Specific storage, Ss (m^{-1})*	Specific yield, Sy (−)	Effective porosity (−)	Total porosity (−)	Longitudinal Dl (m)
Alluvium (Al)	1.10×10^{-7} to 1.10×10^{-5}	1.10×10^{-7} to 1.10×10^{-5}	1.00×10^{-2}	0.30	0.35	0.40	500
Terrace Deposit (Te)	1.00×10^{-5} to 5.00×10^{-2}	5.00×10^{-6} to 5.00×10^{-3}	8.00×10^{-3}	0.25	0.30	0.40	600
Upper phutok (Upt)	3.70×10^{-7} to 1.80×10^{-6}	3.70×10^{-8} to 4.80×10^{-7}	3.00×10^{-3}	0.15	0.25	0.30	150
Lower phutok (Lpt)	1.09×10^{-7} to 2.70×10^{-4}	1.09×10^{-8} to 2.70×10^{-5}	1.70×10^{-3}	0.17	0.22	0.31	70
Rock salt (RS)	2.00×10^{-14}	2.00×10^{-14}	1.00×10^{-5}	0.01	0.02	0.10	50
Khok Kruat (Kk)	7.49×10^{-8} to 5.76×10^{-5}	7.49×10^{-9} to 5.76×10^{-6}	5.00×10^{-3}	0.20	0.25	0.30	70
Lower Khorat Group (Lkg)	5.00×10^{-9} to 5.00×10^{-7}	5.00×10^{-10} to 5.00×10^{-8}	2.00×10^{-3}	0.20	0.25	0.30	150

the years of 2014 to 2015. According to the groundwater usage investigation in the CHLB, there is about 1880 m^3 of water abstracted daily and it is abstracted from various aquifers at about 30%, 25%, 15%, 15%, 10%, and 5% from the Upt, Lpt, Kk, Te, Al, and Lkg units, respectively.

3.1.2. Groundwater recharge estimation

Groundwater recharge rates depend upon the rainfall intensity, temperatures, other weather conditions, slopes, soils, and ground surface covers. In contrast, the recharge rate is subjected to various hydrological processes, such as interception, infiltration, evaporation, and surface run-off. In this study, the Hydrologic Evaluation of Landfill Performance (HELP) computer program (Schroeder et al., 1994) was selected to be used to estimate the groundwater recharge rates. It has also been used to estimate the impact of climate change on the spatial varying groundwater recharge rates in New Jersey (Jyrkama et al., 2002), of the Grand River Watershed (Jyrkama and Sykes, 2007), in the Grand Forks Area (Scibek and Allen, 2006; Scibek et al., 2007) and in the Huai Khamrian subwatershed (Saraphirom et al., 2013a). For a detailed description of

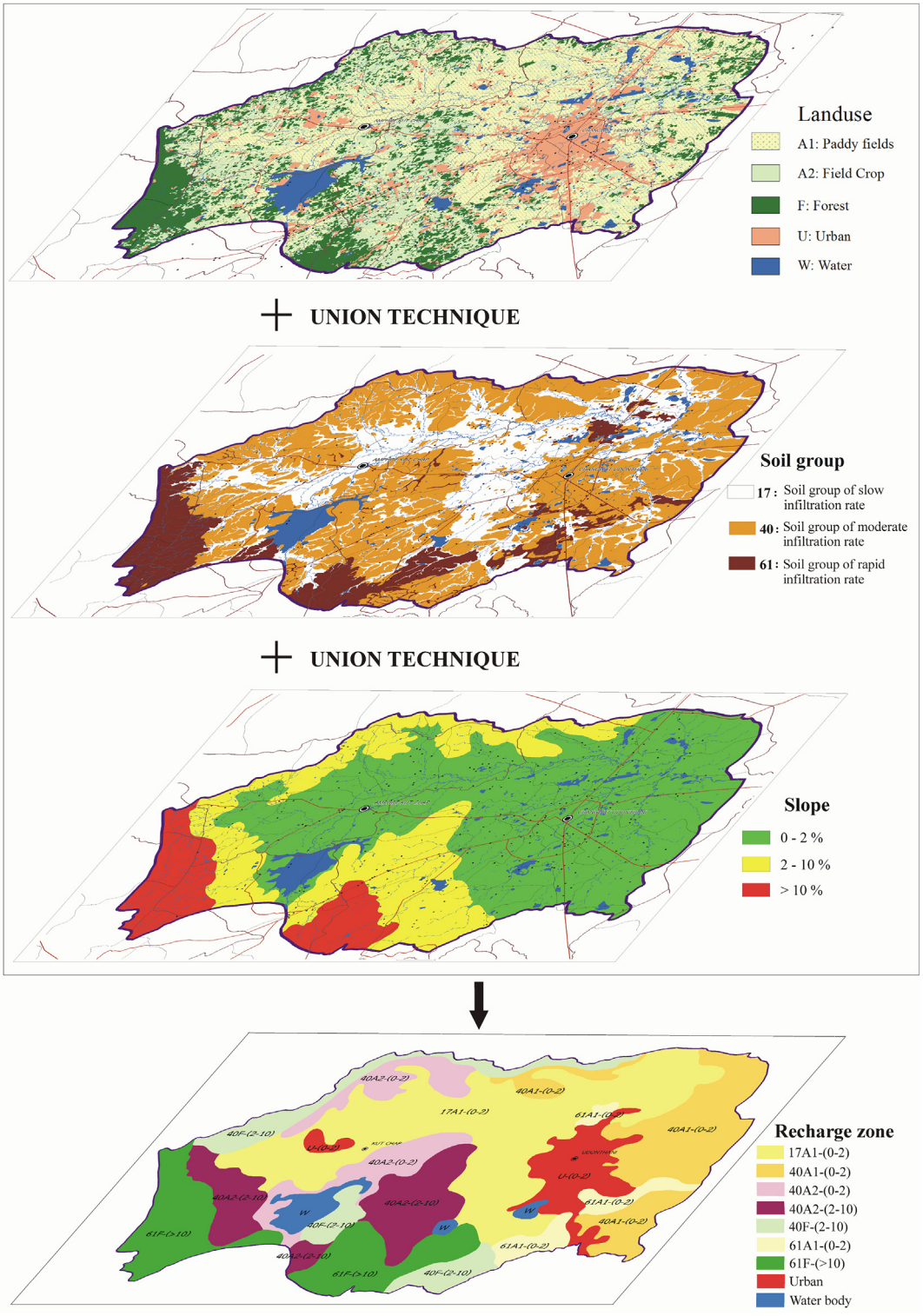

Fig. 5. Recharge zones estimated by an integration of land use, soil types, and topographic slopes.

the HELP model, see Schroeder et al. (1994). The HELP3 model is a quasi-two-dimensional, deterministic water routing model for computing water balances. It simulates the daily movement of water into the ground and accounts for precipitation in any form: surface storage; run-off; evapotranspiration; vegetative interception and growth; unsaturated flow; and temperature effects (Saraphirom et al., 2013a). The water balance method is used to be calculated the net potential recharge as a residual of all of the other water balance components. It is expressed in the following formula:

$$R = P - D - ETa - \Delta W \quad (2)$$

in which R is the potential net recharge (LT^{-1}), P is the precipitation (LT^{-1}), D is the net run-off (LT^{-1}), ETa is the actual amount of evapotranspiration (LT^{-1}), and ΔW is the change in the soil water storage (LT^{-1}).

Various data were required, such as the climate and the soil types, which were used to estimate the water flow through a soil column and which represents the recharge rates of each zone. HELP3 was chosen to cooperate with SEAWAT because it can simulate all of the important processes in the hydrologic cycle in each recharge zone. The recharge rates were used as boundary conditions for groundwater simulations in the watershed scale. The recharge zones in the SEAWAT model were classified by land use, soil type, and by topographic slope as shown in Fig. 5. The soil profile and properties were assigned as a soil column in the HELP3 model (Table 2). Nine recharge zones were assigned to represent each zone. The results from the HELP3 model were used as inputs for each zone in SEAWAT model.

3.2. Future climate scenarios

To examine the projected impact of climate change in the near future, the future climate of the GCMs under the IPCC Fourth and Fifth Assessment Report (AR4 and AR5) were considered. For AR4, the Southeast Asia Climate Analyses & Modeling (SEACAM) regional climate modeling experiment provides high resolution (25 km) information on future climate projections for the Southeast Asia (SEA) region up to the end of this century. This was carried out by the dynamical downscaling of the Met Office HadCM3Q ensemble-based GCMs, which were retrieved from the CMIP3, and by using the Met Office PRECIS model (SEACAM, 2014). The SEACAM climate model was selected to examine the projected impact of climate change on the groundwater quantity and quality in the CHLB due to the fact that it was developed for SEA region, which is particularly vulnerable to weather and climate extremes and is affected by extreme weather events, particularly tropical cyclones, drought, and floods (Weiss, 2009). Large areas of SEA are prone to flooding, and much of the region is heavily influenced by monsoon systems which often bring extreme weather (Yusuf and Francisco, 2009). The SEACAM climate model was used to study the impact of climate change on the SEA member countries, due to the fact that it has been developed by climate change specialists and scientists in their own countries and that it reliably represents future climate. In order to evaluate an appropriate climate model that is able to represent the future climate of the CHLB, visual comparisons and statistical measurements of the observed temperature and the precipitation data of CHLB and SEACAM climate model were analyzed for the baseline period (2006–2015). The results showed that the historical data of SEACAM and the observed data of the baseline period had correlated well. As can be seen from the results of the statistical measurements in Table 3, the findings had been reasonably reliable in representing the future climate of the CHLB.

The SEACAM climate model is available only under AR4, other GCMs under AR5 were explored in order to be selected to represent the future climate of the CHLB for the latest Assessment Report. Ten of the GCMs, including CNRM-CM5, MIROC-ESM, FGOAL-s2, MPI-ESM-LR, CESM1-BGC, CCSM4, CanESM2, HadGEM2-CC, and GFDL, have been widely used in Thailand (Chaowiwat et al., 2017). These are included in IPCC AR5 and were selected to evaluate a suitable climate model. The recorded temperature and precipitation data from the CHLB and from the ten GCMS during the baseline period (2006–2015) was statistically analyzed by the same method used for SEACAM. The results from the visual comparisons and the statistical measurements indicated that the CanESM2 was shown the best correlation when compared to the others, with coefficients of determination (R^2) of 0.67 and 0.68 for average monthly temperature and the average monthly amount of precipitation, respectively. In contrast, other GCMs exhibited coefficients of determination (R^2) at 0.23–0.46 and 0.19–0.49 for the average monthly temperature and the average monthly amount of precipitation, respectively. Therefore, it was found that CanESM2 was reasonably reliable in representing the future climate of the CHLB as shown in the results from the statistical measurements in Table 3. The second generation Canadian Earth System Model (CanESM2) consists of the physical coupled

Table 2
Recharge zone, soil profiles, and other input parameters for estimating of groundwater recharge.

Zone	Layer	Depth (cm)	Soil texture -	Ø (vol/vol)	FC (vol/vol)	WP (vol/vol)	Ks (cm/s)	Slope (%)	Land use	EZD (cm)	LAI
17A1-(0–2)	1	0–20	Loamy fine sand	0.49	0.28	0.14	5.0×10^{-5}	1.00	Rice	56	3
Lowland soil, paddy field, slope 0–2%	2	20–65	Silt	0.48	0.30	0.10	1.9×10^{-6}	–	–	–	–
	3	65–130	Silty loam	0.49	0.28	0.14	1.9×10^{-6}	–	–	–	–
	4	130–200	Silty clay	0.49	0.38	0.22	1.3×10^{-8}	–	–	–	–
40A1-(0–2)	1	0–40	Loamy sand	0.50	0.35	0.20	5.0×10^{-5}	1.50	Rice	56	3
Upland soil, paddy field, slope 0–2%	2	40–90	Silt loam	0.35	0.32	0.20	1.0×10^{-7}	–	–	–	–
	3	90–120	Clay	0.475	0.378	0.256	1.0×10^{-9}	–	–	–	–
	4	120–200	Silty clay loam	0.445	0.393	0.277	3.8×10^{-8}	–	–	–	–
40A2-(0–2)	1	0–200	Sandy loam	0.453	0.19	0.085	7.5×10^{-5}	1.50	Sugar Cane	102	4
Upland, field crop, slope 0–2%	2	150–200	Silty clay	0.479	0.371	0.251	6.15×10^{-8}	–	–	–	–
40A2-(2−10)	1	0–90	Sandy loam	0.45	0.30	0.09	3.85×10^{-6}	5.00	Sugar Cane	102	4
Upland, field crop, slope 2–10%	2	90–200	Gravel	0.45	0.032	0.013	3.0×10^{-1}	–	–	–	–
40F-(2–10)	1	0–90	Silty sand	0.501	0.284	0.135	1.9×10^{-5}	5.00	Forest	102	7
Upland, forest, slope 2–10%	2	90–120	Silty sand and Laterite	0.463	0.232	0.116	3.5×10^{-6}	–	–	–	–
	3	120–200	Clay	0.475	0.378	0.265	3.0×10^{-9}	–	–	–	–
61A1-(0–2)	1	0–150	Sandy loam	0.453	0.19	0.085	1.0×10^{-5}	1.75	Rice	102	7
Highland soil, paddy field, slope 0–2%	2	150–200	Silty clay	0.479	0.371	0.251	3.15×10^{-8}	–	–	–	–
61F-(>10)	1	0–100	Loamy sand	0.437	0.105	0.047	1.7×10^{-3}	15.00	Forest	102	7
Highland soil, forest, slope > 10%	2	100–150	Gravel	0.397	0.032	0.013	1.0×10^{-1}	–	–	–	–
	3	150–200	Clay	0.475	0.378	0.25	2.73×10^{-8}	–	–	–	–
Water body	–										
Urban	–										

Remarks: leaf area index (LAI), evaporative zone depth (EZD), total porosity (Ø), field capacity (FC), wilting point (WP), and saturated hydraulic conductivity (KS).

Table 3
A summary of the statistics of the observed and simulated historical data for the CHLB during the period 2006–2015.

	Monthly average temperature (°C)		Monthly average precipitation (mm)	
	SEACAM	CanEMS2	SEACAM	CanEMS2
SD, Obs	2.49	2.49	110.99	110.99
SD, Sim	3.63	2.85	84.83	95.94
Mean, Obs	26.98	26.98	105.72	105.72
Mean, Sim	28.36	27.99	87.15	111.56
Median, Obs	27.80	27.80	66.53	66.53
Median, Sim	29.34	28.66	60.08	67.90
R^2 (coefficient of determination)	0.72	0.67	0.63	0.68

atmosphere-ocean model (CanCM4) coupled with a terrestrial carbon model (CTEM) and an ocean carbon model (CMOC) (Chylek et al., 2011). GCM precipitation and temperature were downloaded and downscaled using the PRECIS model. The Gamma-gamma (GG) transformation with the optimizing parameter method was adopted to downscale the temperature and the precipitation from the global scale to the river basin scale. The characteristics of the gamma cumulative density function (CDF) were used to remove the biases from the RCM precipitation data (Chaowiwat et al., 2017) and to provide information with higher resolution (10 km) for future climate projections.

Four of SEACAM downscaled climate scenarios of HadCM3Q3, HadCM3Q10, HadCM3Q11, and HadCM3Q13 were selected in order to investigate the potential impact of future climate scenarios on groundwater and its consequences on waterlogging and salinity distribution in the CHLB. In capturing the Asian monsoons, the HadCM3Q3 model showed the lower degree of temperature change, while the HadCM3Q13 model showed the higher degree of temperature change for the SEA regions. During the wet seasons, the HadCM3Q10 model showed increases in rainfall, while the HadCM3Q11 model indicated decreases in rainfall.

The CanESM2 downscaled climate scenarios, which were used to investigate the impact of groundwater on the CHLB, were the Representative Concentration Pathways (RCPs) 4.5 and 8.5 which were presented in the AR5 of IPCC. The RCP 8.5 is the highest emission that is considered to be consistent with the future of no policy changes to reduce emissions. It was developed by the International Institute for Applied System Analysis in Austria and is characterized by increasing greenhouse gas emissions that lead to high greenhouse gas concentrations over time. The RCP 4.5 represents the intermediate emissions developed by the Pacific Northwest National Laboratory in the US. Here, radiative forcing is shown to be stabilized shortly after 2100, which is consistent with the future of relatively ambitious reductions in emissions.

Selected future climate scenarios in this study was summarized in Table 4.

3.3. Climate change impacts on groundwater resources assessment

The impact of climate change on groundwater resources affects recharge rates, patterns, and timing; decreases/increases in groundwater levels; and the deterioration of groundwater quality (e.g., Shrestha et al., 2016; Pratoomchai et al., 2014; Saraphirom et al., 2013a; Jyrkama and Sykes, 2007). The impact on the groundwater resources for this study was investigated by examining the changes in groundwater recharges, levels, flow patterns, and salinity as indicators of groundwater storage, waterlogging, and salinity distribution.

During the period from 2010 to 2015, the models, HELP3 and SEAWAT, were calibrated and validated with the observed groundwater levels and salinity levels. Simulations of groundwater flow and salt transport under the future climate data of 4 SEACAM scenarios and 3 CanESM2 scenarios were projected for the next 30 years. The climate data was used as the input data in the HELP3 model to estimate the net recharge from 2016 to 2045. Then the projected groundwater recharge for each scenario was used as the recharge input for the SEAWAT model in order to simulate the groundwater levels, flow patterns, and salinity distributions.

The impact of climate change on the groundwater resources was classified in terms of groundwater quantity and quality. The differences in groundwater storage values from the aquifer balance between the baseline and future periods were utilized to assess the impact upon groundwater quantity. Differences were found in areas in which the depths of water table can move upward towards the soil surface and can cause the accumulation of salt (waterlogging). Moreover, groundwater salinity changes between the baseline and future periods were used to assess the impact on groundwater quality. The waterlogging and salinity distributions were evaluated by means of the areal distribution of the water table depths and the expansion of the saline groundwater boundaries.

4. Results and discussion

4.1. Baseline groundwater flow situation

The groundwater condition of the CHLB in the baseline period (2006 to 2015) was simulated. The hydraulic heads and salinity of the 89 wells, distributed in six aquifers in the CHLB, were measured from September 2014 to December 2015 and were used as calibrated data. The model was validated with 33 observation wells which had been monitored during the years from 2010 to 2012. The model performance was evaluated by making visual comparisons of the groundwater levels and salinity in terms of Total Dissolved Solid (TDS) between the observed versus the simulated both groundwater level and TDS and by using the Root Mean Square error (RMSE) and the Normalized RMSE (NRMSE) as statistical measurements (Table 5 and Fig. 6). Major groundwater flow directions have been replicated for the topographic terrain as presented in the hydrogeologic map (Fig. 6). The comparison of simulated and observed hydraulic heads and TDS is reasonable. Sensitivity analyses of the groundwater flow and salt transport model, the SEAWAT model, were carried out in order to study the sensitivity of the recharge rates, the hydraulic conductivity, the storage coefficients, the dispersivity, and the effective porosity of the groundwater level and salinity. The results indicated that the recharge rates had been the most sensitive parameters for the ground water level (Fig. 7(a)), while the dispersivity had been the most sensitive parameter for groundwater salinity (Fig. 7(b)). The water balance in 2015 showed that water inflow

Table 4
Selected future climate scenarios in this study (SEACAM, 2014; van Vuuren et al., 2011).

Model	IPCC	Downscale resolution	Scenarios	Description
SEACAM	AR4, CMIP3	25 km × 25 km	HadCM3Q3	Simulates lower degree of temperature change in the future in SEA region, HadCM3 GCM and downscaling by PRECIS
			HadCM3Q13	Simulates higher degree of temperature change in the future in SEA region, HadCM3 GCM and downscaling by PRECIS
			HadCM3Q10	Simulates rainfall decreases in the future in SEA region (dry), HadCM3 GCM and downscaling by PRECIS
			HadCM3Q11	Simulates rainfall increases in the future in SEA region (wet), HadCM3 GCM and downscaling by PRECIS
CanESM2	AR5, CMIP5	10 km × 10 km	RCP 4.5	Stabilization without overshoot pathway to 4.5 W/m^2 at stabilization after 2100, CanESM2 GCM and downscaling by PRECIS
			RCP 8.5	Rising radiative forcing pathway leading to 8.5 W/m^2 in 2100, CanESM2 GCM and downscaling by PRECIS

Table 5
Model performance during calibration and validation.

		Root Mean Squared Error	Normalized RMSE
Calibration	Hydraulic head (m)	2.28	3.03%
	TDS (mg/l)	529.39	1.35%
Validation	Hydraulic head (m)	2.99	4.14%
	TDS (mg/l)	444.35	3.22%

to the aquifers from groundwater recharge and river leakage had been about 97.01 MCM/year, while the outflow from the aquifers through wells abstraction, river leakage, and GHB had been only 13.67 MCM/year. It was found that the inflow to the aquifers was greater than the water outflow from the aquifers at about 83.4 MCM/year. Therefore, the groundwater levels had tended to increase in the year of 2015.

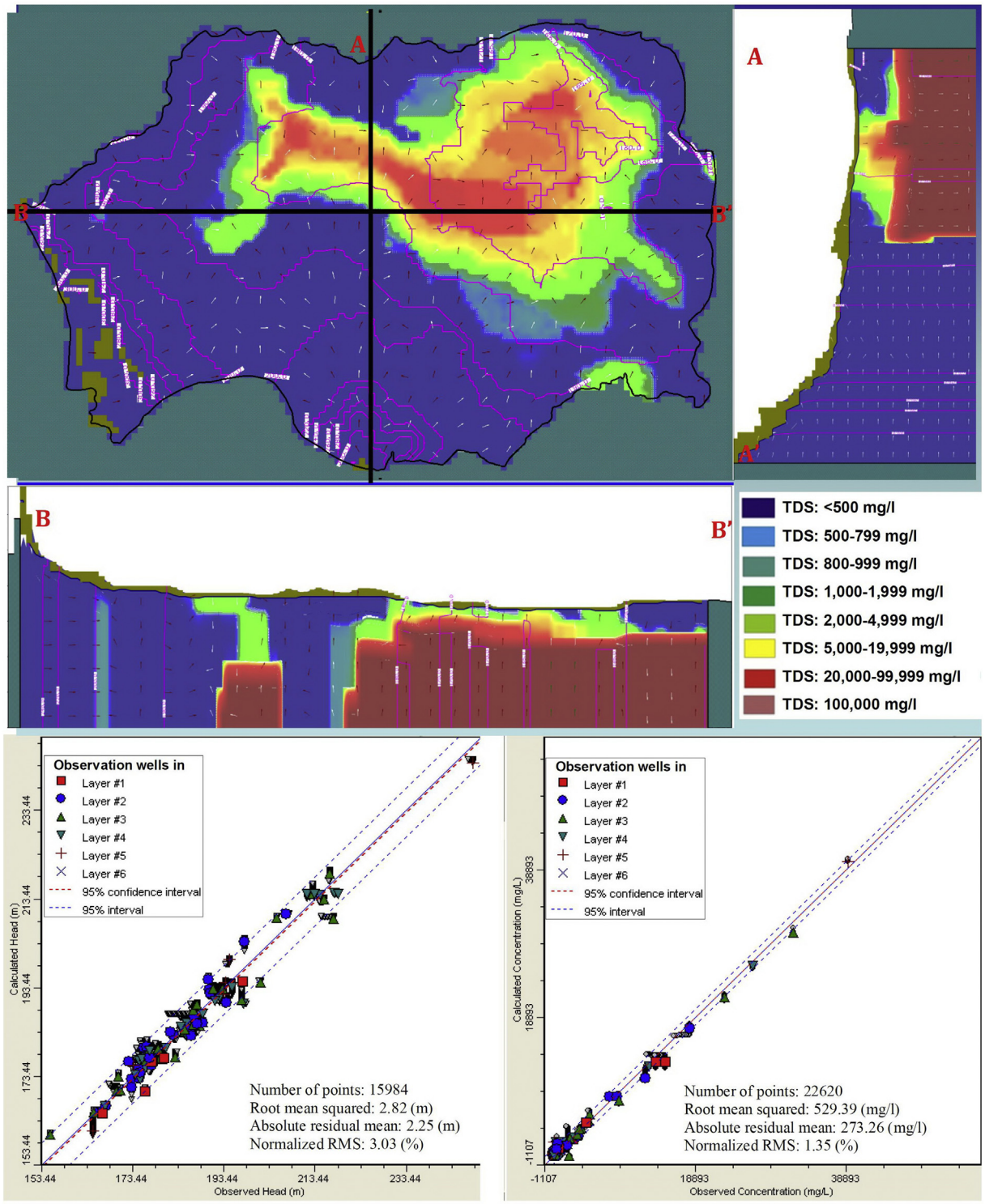

Fig. 6. Simulated groundwater flow and salinity distribution for the current situation and the calibration results.

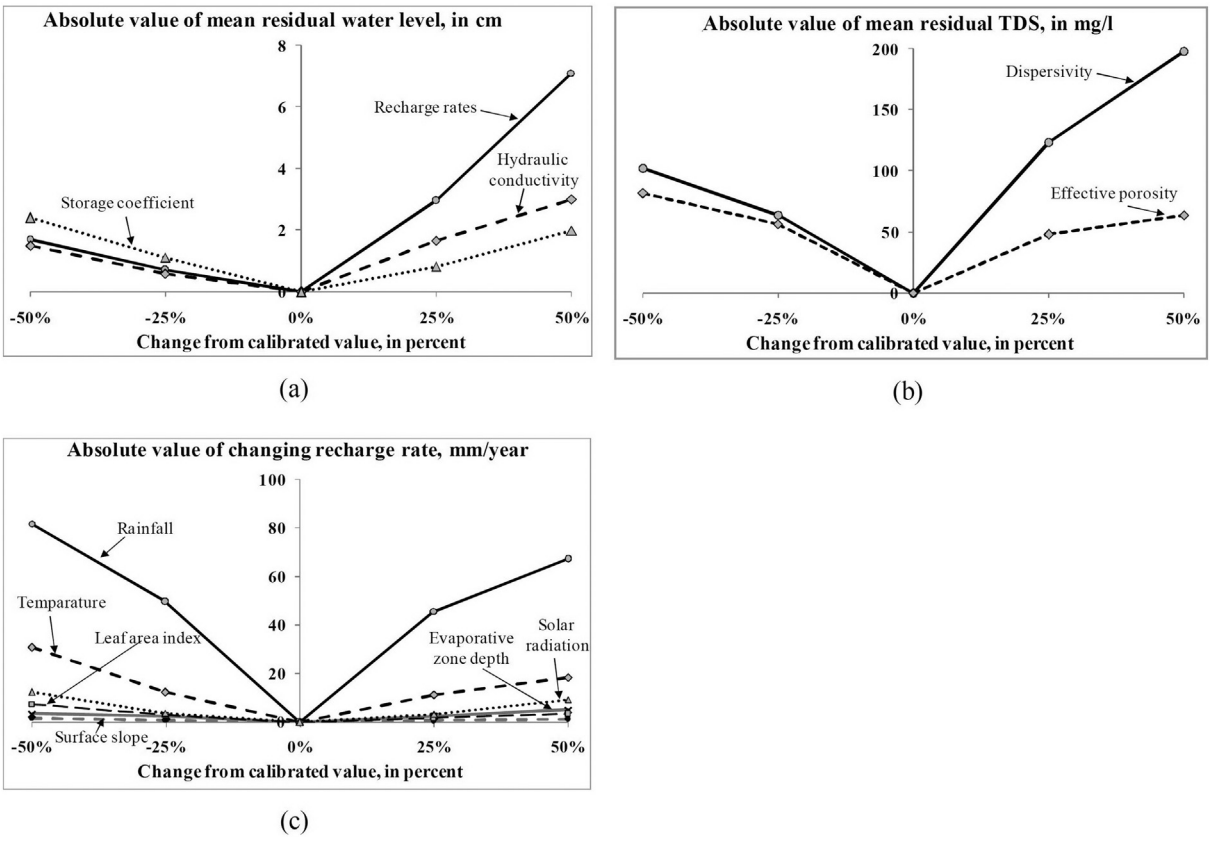

Fig. 7. A Sensitivity analysis of the calibrated models: (a) a sensitivity analysis of groundwater level in SEAWAT model (b) a sensitivity analysis of groundwater salinity in SEAWAT model, and (c) a sensitivity analysis of the HELP model.

4.2. Baseline groundwater recharge situation

The groundwater recharge model, HELP3, was calibrated together with the SEAWAT in order to estimate the spatially distributed, long-term average recharge rates in the CHLB. The HELP3 model was used to estimate the recharge volume of each recharge zone using the water balance concept. The HELP3 model parameters, that gave the recharge rates which were used to satisfactorily calibrate the SEAWAT model, were considered as the final recharge rates estimated by HELP3. As shown in Table 6, the results indicated that the recharge rates had varied from 0% to 15.25% of rainfall in the discharge areas to the recharge areas, respectively. The simulations under the baseline conditions showed that the average annual recharge was around 98.36 MCM and almost 90% of the recharge had taken place during the wet season (May to October). A sensitivity analysis of the recharge estimation model was carried out in order to investigate the sensitivity of the input climate parameters and variables in the HELP model. Climate parameters, namely precipitation, temperature and solar radiation indicated more sensitive than variables include, leaf area index, evaporative zone depth and surface slope. The results showed that precipitation was the most sensitive parameter, followed by temperature (Fig. 7 (c)). In contrast, the solar radiation and other variables were not found to be sensitive and not to have much of an influence on recharge rate estimation.

4.3. Baseline of groundwater salinity and waterlogging situation

In order to analyze the impact on water abstraction availability, the potential of waterlogging, and the distribution of soil salinity, the baseline of the groundwater conditions in the CHLB were analyzed into two systems: the shallow and deep groundwater systems. The 1st model layer, representing the shallow groundwater system, was selected to analyze the potential effects on top soil salinity for current and future scenarios using the depth of the water table and salinity. Due to the fact that groundwater is generally extracted from depths of >20 m below the ground surface, the deep groundwater system in this study was represented by the 3rd model layer. In this study, the salinity of the groundwater was classified into 3 ranges based on TDS values: 1000–5000 mg/l, 5000–20,000 mg/l, and >20,000 mg/l. The reason for this classification is that groundwater, which has a TDS of higher than 1000 mg/l, has the potential of making the soil become saline soil when it rises to the ground surface.

Saline shallow groundwater, which has the potential to affect the salinity of top soil, covers an area of 205 km^2 or 13.8% of the CHLB (Fig. 8 (a)). The waterlogging area (water table <4 m) covers an area of about 567 km^2 or 37.08% of the CHLB with 3 ranges of water table depth (Fig. 8 (a)). Deep saline groundwater has been placed into 3 levels as shown in

Table 6
Average annual groundwater recharge rates of the baseline period in each recharge zone.

Recharge zones	Name	Average annual recharged water mm/year (% of the rainfall)	Average annual recharged water MCM/year
Zone 1	17A1-(0-2)	10.48 (0.75)	4.64
Zone 2	40A1-(0-2)	25.40 (2.0)	5.81
Zone 3	40A2-(0-2)	48.28 (4.75)	5.83
Zone 4	40A2-(2-10)	160.18 (12.75)	27.19
Zone 5	40F-(2-10)	105.96 (8.25)	13.52
Zone 6	61A1-(0-2)	35.33 (3.10)	1.97
Zone 7	61F-(>10)	190.98 (15.25)	39.38
Zone 8	Urban	0.18 (0.015)	0.02
Zone 9	Water body	0 (0)	0

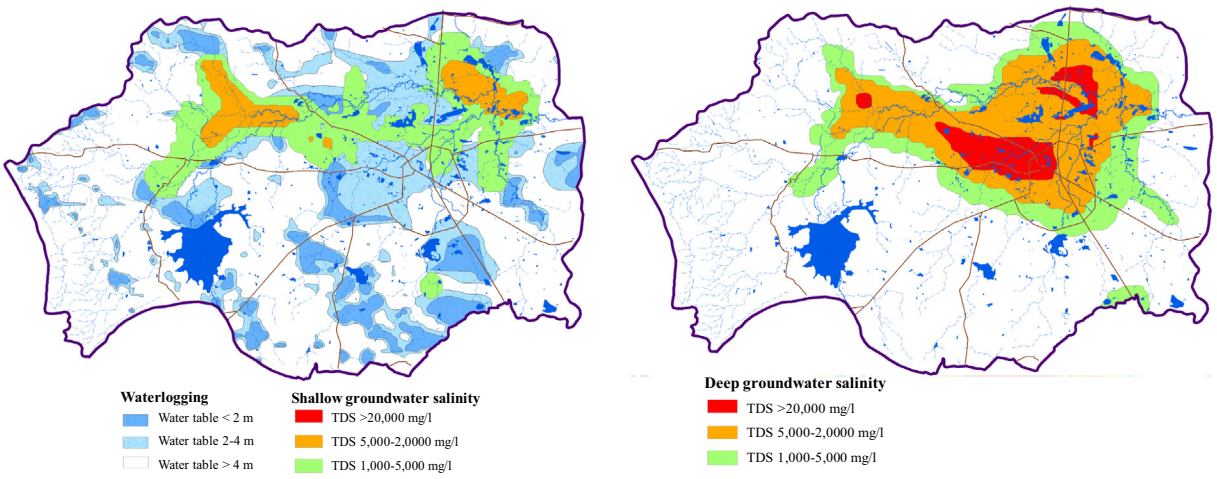

(a) Waterlogging and shallow groundwater salinity

(b) Deep groundwater salinity

Fig. 8. Waterlogging and shallow saline groundwater areas (a), and deep groundwater salinity (b) under baseline conditions.

Fig. 8(b) and can be found in the flood plain of the Huai Luang River and in the surrounding areas. Its area is about 435.77 km^2 or 28.50%.

4.4. Future climate conditions

4.4.1. Projected future temperature

The projected average annual temperatures from the SEACAM and CanESM2 climate models for the years from 2016 to 2045 and their decades periods compared to baseline period (2006–2015) have indicated that the average annual temperatures of both models are higher than the baseline period for all scenarios. Furthermore, a significant trend, showing gradual increases from year by year, was discovered (Table 7). It is clear that average annual temperatures of CanESM2 are less than SEACAM in every scenario except the HadCM3Q3 (low) scenario. The HadCM3Q10 (dry) scenario of SEACAM had the highest average annual temperature for each time period. Compared to the RCP 4.5 scenario, the temperatures from the RCP 8.5 scenario were not found to have significantly changed. By the year 2045, the average annual temperatures are projected to increase by 3.5 °C, 1.5 °C, 3.4 °C, 4.0 °C, 1.7 °C, and 2.7 °C under the HadCM3Q13 (high), HadCM3Q3 (low), HadCM3Q10 (dry), HadCM3Q11 (wet), the RCP4.5, and the RCP8.5 scenarios, respectively. Fig. 9(a) and (b) show that for all scenarios the average monthly temperatures will increase for every month.

4.4.2. Projected future precipitation

Projected annual rainfall from the SEACAM and CanESM2 climate models for years from 2016 to 2045 and their decades periods (compared to baseline period) show that the annual rainfall of SEACAM is lower than the baseline for all scenarios. In contrast, the annual rainfall of CanESM2 is higher than the baseline period for all scenarios (Table 7). It is clear that annual rainfall of CanESM2 will be higher than SEACAM for every scenario. The trend for the annual rainfall of SEACAM is to increase from 2016 to 2045. The HadCM3Q13 (high) and HadCM3Q11 (wet) scenarios show a higher annual rainfall than HadCM3Q3 (low) and HadCM3Q10 (dry) during almost every time period. The RCP 8.5 scenario of the CanESM2 model projected the highest annual rainfall. The annual rainfall from the CanESM2 model showed a gradually increasing trend from 2016 to 2025 and from 2026 to 2035. It then showed a slight decrease in the last period (2036–2045) of this projection. By 2045, the annual rainfall was projected to decrease by 4.8%, 14.4%, 18.7%, and 7.4% under the HadCM3Q13 (high), HadCM3Q3 (low), HadCM3Q10 (dry), and under the HadCM3Q11 (wet) scenarios, respectively. Meanwhile, under the RCP4.5 scenario, annual rainfall was projected to increase by 6.9% and by 10.7% under the RCP8.5 scenario.

Rainfall regime in the CHLB has a distinct wet season (May to October) and dry season (November to April). Rainfall changes during the wet seasons are more distinct compared to the dry seasons. Seasonal rainfall will change significantly in the dry season, and rainfall will decrease by 33.1% under SEACAM model and increase by 30.5% under the CanESM2 models when compared to the baseline. Mean monthly rainfall from SEACAM will not change significantly compared to the baseline until the months of June, July, and August. It showed that the highest amounts of rainfall were to be contributed during the year from August to June and in September (Table 8 and Fig. 9(c)). This change will lead to greater distributions of rainfall to other months in the wet season.

The mean monthly rainfall of CanESM2 model showed that rainfall in the wet season is expected to increase significantly in May and June, whereas, under all the scenarios, it is projected to decrease slightly during the months of July and August (Table 8 and Fig. 9(d)). In regard to the mean monthly rainfall of the SEACAM model, a greater

Table 7
Future precipitation and temperature scenarios projected by SEACAM and CanESM2 climate models.

Year		Baseline (2006–2015)	SEACAM				CanESM2	
			HadCM3Q13 (high)	HadCM3Q3 (low)	HadCM3Q10 (dry)	HadCM3Q11 (wet)	RCP 4.5	RCP 8.5
2016–2045	P (mm)	1268.6	1207.8	1086.2	1031.8	1174.8	1356.6	1404.7
	T (°C)	27.0	29.1	28.18	29.51	29.41	28.64	28.77
2016–2025	P (mm)	1268.6	1056.3	957.1	1091.7	1094.0	1301.5	1303.4
	T (°C)	27.0	28.66	27.83	28.75	28.84	28.40	28.45
2026–2035	P (mm)	1268.6	1239.6	1091.8	1083.1	1256.4	1426.6	1482.8
	T (°C)	27.0	28.99	28.17	29.50	29.25	28.44	28.80
2036–2045	P (mm)	1268.6	1242.6	1142.8	1042.9	1154.4	1322.6	1410.5
	T (°C)	27.0	29.76	28.54	30.27	30.14	29.08	29.07

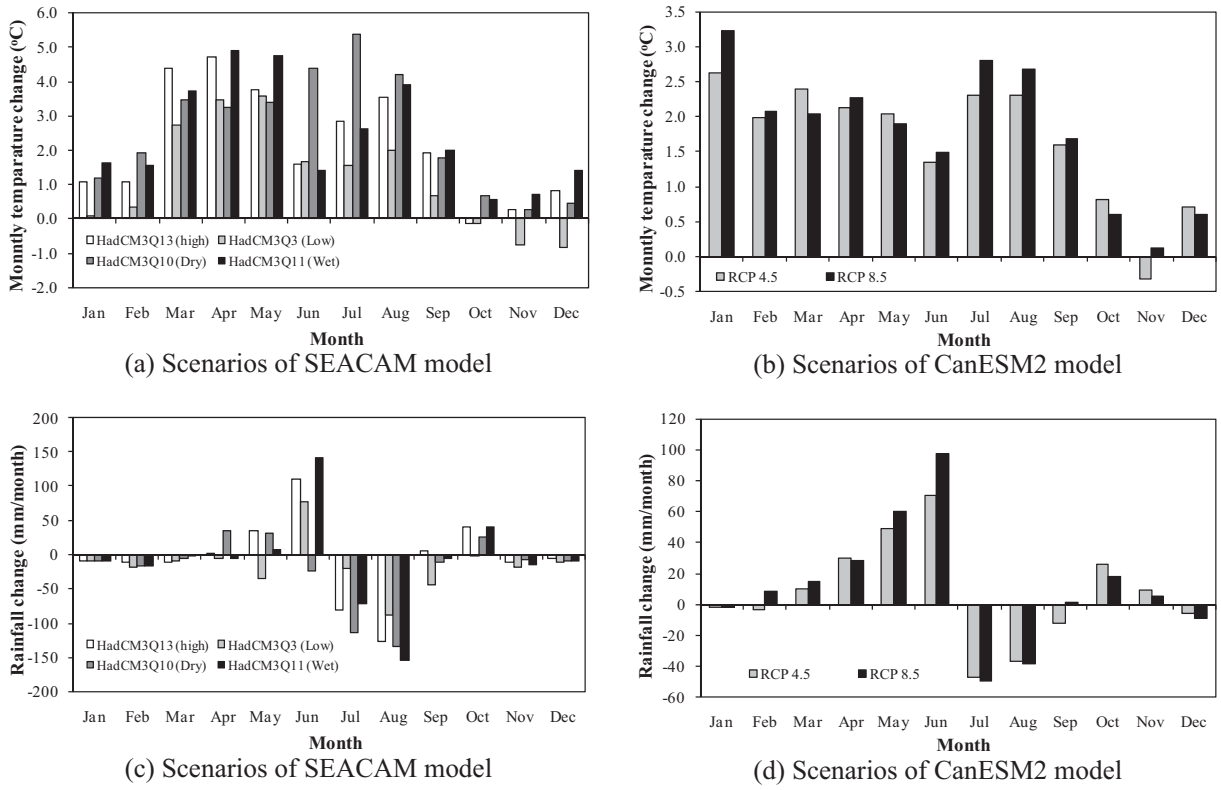

Fig. 9. Changes in average monthly temperature (a and b) and mean monthly rainfall (c and d) against baseline under SEACAM and CanESM2 climate models.

distribution of rainfall was indicated in the months of the wet season as compared to the baseline. During the dry seasons of the next 30 years, rainfall is projected to significantly increase under all scenarios.

4.5. Impact of climate change on groundwater resources

Climate change has resulted in an alteration of the water balance in the CHLB. The means by which the groundwater recharge and storage are projected to be altered in both quantity and quality under future climatic conditions is discussed below:

4.5.1. Impact of climate change on groundwater recharge and storage

The calibrated HELP3 model was used to predict future groundwater recharge by 2045 under SEACAM and CanESM2 climate conditions. The result showed that the annual groundwater recharge was projected to increase under the CanESM2 future climate conditions (Table 9 and Fig. 10). The annual recharge of the SEACAM's scenarios will decreases from the baseline during 2016–2025 and then increases towards 2045 with the exception of the HadCM3Q10 (dry) scenario, while the CanESM2's scenarios will increase from the baseline period. By 2045, the groundwater recharge in the CHLB was projected to increase by about 3.98%, 6.29%, 15.21%, and 18.90% compared to the baselines under the HadCM3Q13 (high) and HadCM3Q11 (wet) scenarios of the SEACAM, and the RCP 4.5, and RCP 8.5 scenarios of the CanESM2, respectively. In contrast, the simulated groundwater recharge under the HadCM3Q3 (low) and HadCM3Q10 (dry) were expected to decrease by about 0.57% and 12.39% compared to baseline by 2045. Groundwater recharges under future climate conditions in the wet and dry seasons are also presented in Table 9. The projected recharge in the wet season of the SEACAM is expected to increase from 89.28% of annual recharge for the baseline to around 93.23% under all scenarios. The results will be a greater distribution of rainfall in the wet seasons and a decrease of rainfall in the dry seasons. This means that the recharge in the dry seasons will contribute less, which corresponds well to the decrease in projected rainfall during the dry season of the SEACAM model. The proportion of recharge between wet seasons under the CanESM2 model is around 84.41% of annual recharge, which shows a decrease from baseline. This is due to an increase in projected rainfall during the dry seasons.

The projected future recharge under the SEACAM and CanESM2 climate condition were input into the SEAWAT model in order to simulate future groundwater storage. As per the model, the water inflow to the aquifers is more than water outflow from the aquifers and varies from 74.23 to 118.11 MCM/year. This means that the groundwater levels tend to increase annually for all scenarios. When comparing the changes in storage between baseline and the future, the changes in aquifer storage are shown to increase from the baseline in almost every scenario (except HadCM3Q10 (dry) scenario) and in every time period as

Table 8
The projected amounts of monthly rainfall in 10 year periods in the CHLB based upon the SEACAM and CanESM2 climate models.

	Jan	Feb	Mar	Apr	May	Jun	Jul	Aug	Sep	Oct	Nov	Dec	Annual
Baseline	10.1	20.2	23.3	50.8	156.6	143.9	219.2	304.2	239.9	65.8	22.0	12.6	1268.6
CanESM2_2025	7.0	19.9	31.1	73.3	189.7	197.0	151.0	278.7	234.0	81.9	34.3	4.5	1302.4
CanESM2_2035	9.3	22.1	39.5	100.8	262.4	240.3	195.5	272.4	210.8	70.5	26.4	4.6	1454.6
CanESM2_2045	11.3	25.7	38.8	75.3	202.6	227.9	154.8	247.3	253.5	100.8	25.0	3.5	1366.5
SEACAM_2025	0.9	3.7	15.8	49.9	167.1	193.9	149.7	182.5	202.1	69.6	12.7	1.8	1049.7
SEACAM_2035	2.2	5.0	15.8	66.0	160.0	230.8	157.9	191.2	229.0	98.6	8.4	3.0	1167.9
SEACAM_2045	0.9	6.2	13.9	58.9	172.6	214.1	144.1	162.6	254.8	108.5	6.9	2.1	1145.6

Table 9
Simulation of future annual and seasonal groundwater recharge under SEACAM and CanESM2.

Scenarios	Seasonal	Groundwater recharge							
		Baseline		2016–2025		2026–2035		2036–2045	
		MCM	%	MCM	%	MCM	%	MCM	%
HadCM3Q13 (high)	Wet	87.82	89.29	86.02	92.12	106.30	94.35	95.63	94.89
	Dry	10.54	10.71	7.36	7.88	6.37	5.65	5.15	5.11
	Annual	98.36	100.00	93.38	100.00	112.66	100.00	100.78	100.00
HadCM3Q3 (low)	Wet	87.82	89.29	73.76	92.11	95.40	93.41	102.94	92.56
	Dry	10.54	10.71	6.32	7.89	6.73	6.59	8.27	7.44
	Annual	98.36	100.00	80.07	100.00	102.14	100.00	111.21	100.00
HadCM3Q10 (dry)	Wet	87.82	89.29	81.47	91.98	83.58	92.43	74.16	93.24
	Dry	10.54	10.71	7.10	8.02	6.85	7.57	5.37	6.76
	Annual	98.36	100.00	88.57	100.00	90.42	100.00	79.53	100.00
HadCM3Q11 (wet)	Wet	87.82	89.29	91.09	94.66	106.93	93.28	96.49	93.87
	Dry	10.54	10.71	5.14	5.34	7.70	6.72	6.30	6.13
	Annual	98.36	100.00	96.23	100.00	114.63	100.00	102.79	100.00
CanESM2_RCP 4.5	Wet	87.82	89.29	93.02	86.27	102.19	85.43	96.45	85.72
	Dry	10.54	10.71	14.81	13.73	17.43	14.57	16.06	14.28
	Annual	98.36	100.00	107.83	100.00	119.62	100.00	112.52	100.00
CanESM2_RCP 8.5	Wet	87.82	89.29	94.79	86.83	110.71	87.97	98.72	85.23
	Dry	10.54	10.71	14.37	15.17	15.14	12.03	17.11	13.77
	Annual	98.36	100.00	109.16	102.00	125.86	100.00	115.83	99.00

shown in Fig. 6. By 2045, the simulated groundwater storage in the CHLB was expected to increase from baseline at about 17.20%, 11.97%, 20.17%, 28.76%, and 32.06% under HadCM3Q13 (high), HadCM3Q3 (low), and HadCM3Q11 (wet) scenarios of the SEACAM model, the RCP 4.5 scenario and the RCP 8.5 scenario of the CanESM2 model, respectively. Whereas, due to lowest precipitation and recharge, the simulated groundwater storage under HadCM3Q10 (dry) was expected to decrease by 2045 at about 3.66% compared to baseline.

The future groundwater recharge is the most significant aspect that controls aquifer storage in the CHLB and corresponds well to decreases or increases in the projected groundwater storage. The volume and pattern of rainfall for both future climates will conduct the amounts of groundwater recharge.

4.5.2. Impact of climate change on saline groundwater and waterlogging distribution

In every scenario, the results indicated that areas of deep saline groundwater will gradually increase at almost same rate throughout 2045. The area with the highest salinity (TDS > 20,000 mg/l) will tend to decrease, while the moderate salinity (TDS about 5000–20,000 mg/l) and low salinity (TDS about 1000–5000 mg/l) areas will tend to increase (Fig. 11(a)). The spatial aspects of the deep saline groundwater distribution showed that the area of the highest salinity area will become diluted and will, thereby, become an area of moderate salinity. Moreover, the low salinity area will expand to become a non-salinity area (Fig. 12(b)). The projected deep groundwater salinity area under CanESM2 showed a greater increase than the SEACAM, with the highest increase being under RCP 8.5. By 2045, the deep saline groundwater area was projected to increase by 4.67%, 6.17%, 6.12%, and 6.2% compared with baseline under the HadCM3Q13 (high), HadCM3Q3 (low), HadCM3Q10 (dry), and the HadCM3Q11 (wet) scenarios of the SEACAM, respectively. Under the RCP4.5 and RCP8.5 scenarios of CanESM2, there will be increases of 11.97 and 13.31%, respectively. The deep saline groundwater areas will expand from flood plain of the Huai Luang River to the discharge areas.

The future shallow saline groundwater showed a similar trend with deep saline groundwater, it will increase in every scenario and for each level of salinity at almost same rate until the year of 2045. The projected

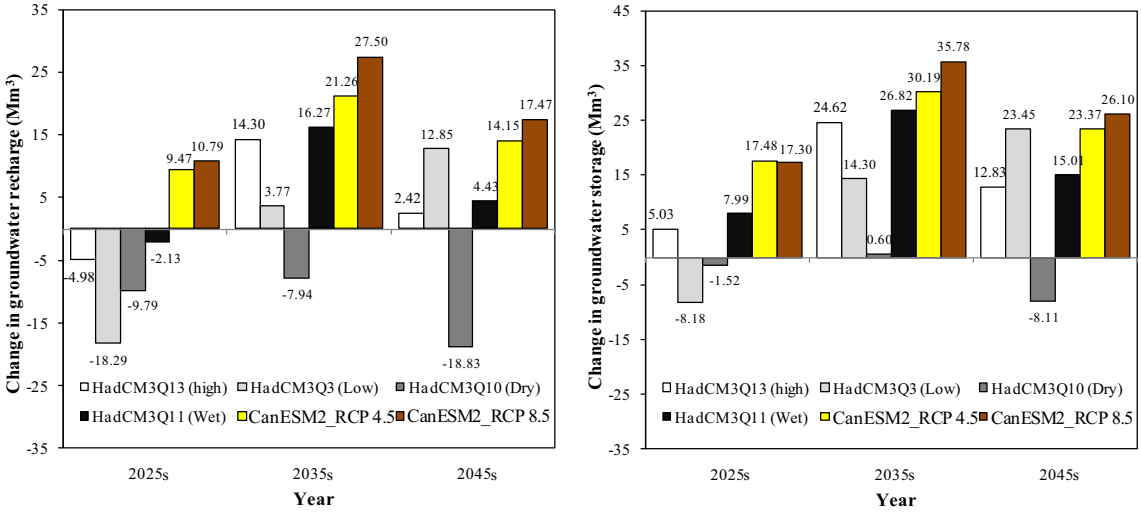

(a) Change in groundwater recharge (b) Change in groundwater storage

Fig. 10. Changes in projected annual groundwater recharge and groundwater storage under SEACAM and CanESM2 climate models.

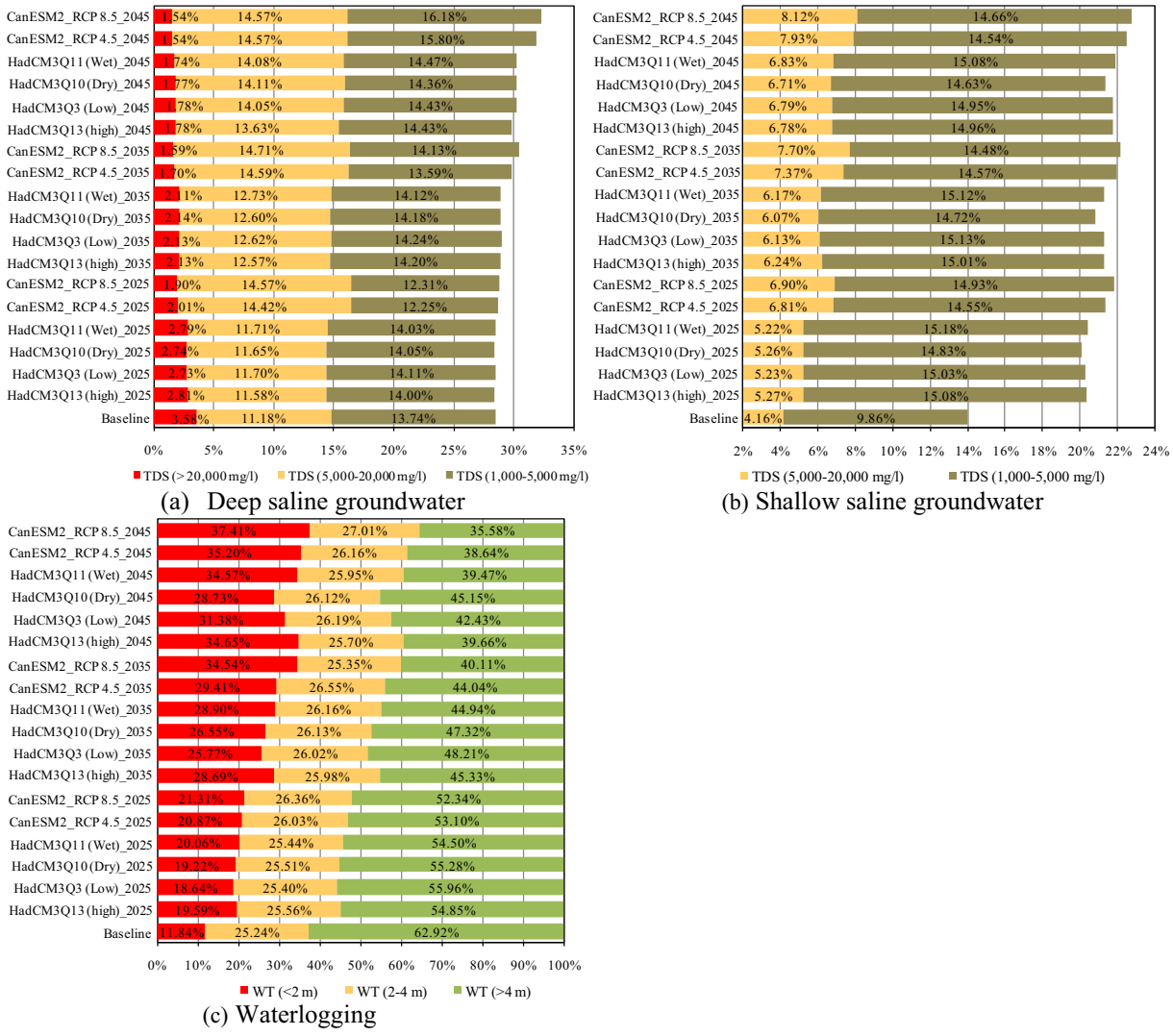

Fig. 11. Percentage of areas with groundwater salinity and waterlogging distribution under the SEACAM and CanESM2 climate models.

shallow groundwater salinity area under CanESM2 was expected to increase more than under SEACAM with the most increases under RCP 8.5. The SEACAM climate conditions indicated that the shallow saline groundwater will increase from the baseline condition by 55.07%, 55.06%, 52.26%, and 56.33% compared to the baseline under HadCM3Q13 (high), HadCM3Q3 (low), HadCM3Q10 (dry), and

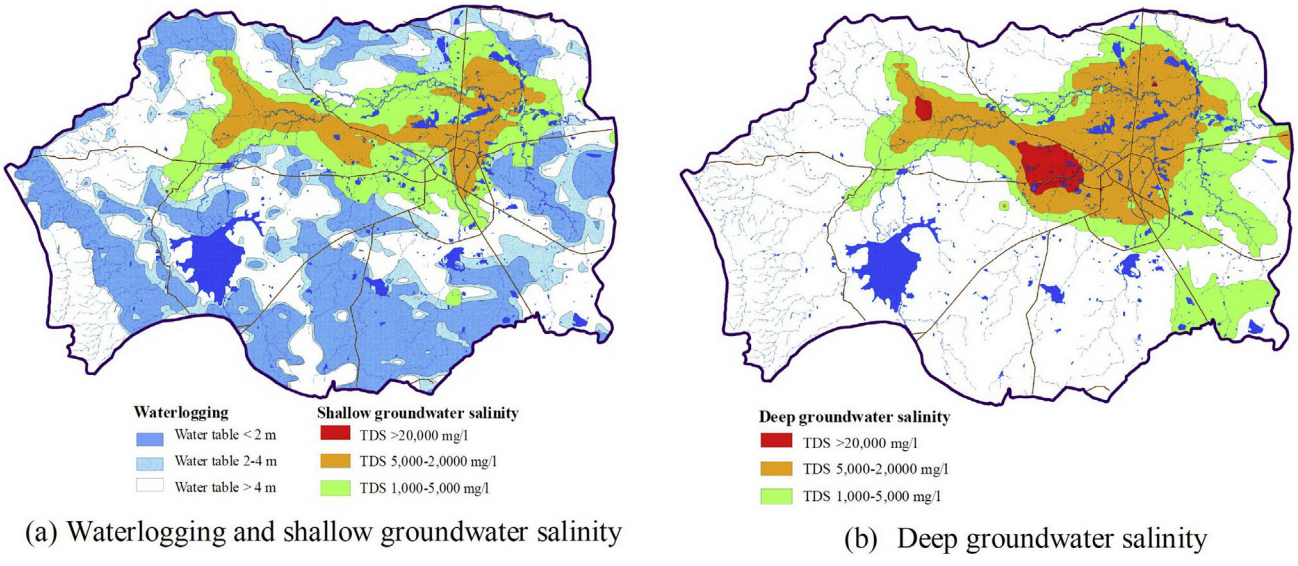

Fig. 12. Waterlogging and shallow saline groundwater areas (a), and deep groundwater salinity (b) under the RCP 8.5 scenario of the CanESM2 climate conditions.

HadCM3Q11 (wet) scenarios, respectively. In contrast, the CanESM2 climate conditions will be 60.28% and 62.49% compared to the baselines under the RCP4.5 and RCP8.5 scenarios (Fig. 11(b)). The shallow saline groundwater areas will also expand from the flood plains of the Huai Luang River to the discharge areas (Fig. 12(a)).

In all climate scenarios, the waterlogging areas will gradually increase. Moreover, the projected waterlogging areas under CanESM2 showed greater increases than the SEACAM. The increases in the groundwater storage conducts to the ringing of the groundwater level and may cause an expansion of waterlogging areas. The waterlogging area tends to extend from the discharge to the recharge areas in some areas (Fig. 12(a)). By 2045, the waterlogging area has been projected to increase by 62.73%, 61.51%, 55.25%, and 63.23% compared to the baselines under the HadCM3Q13 (high), HadCM3Q3 (low), HadCM3Q10 (dry), and HadCM3Q11 (wet) scenarios of the SEACAM, respectively. Furthermore, under the RCP4.5 and RCP8.5 scenarios of CanESM2, increases of 65.46% and 73.73% are expected, respectively (Fig. 11(c)). The projected areas of waterlogging with saline groundwater (TDS > 1000 mg/l), which will affect soil salinity, are expected to increase for both climate conditions.

In every scenario, the projected impact of future climate change on deep groundwater salinity, shallow groundwater salinity, and waterlogging is anticipated to significantly increase. This is especially evident in the RCP 8.5 scenario, which showed the highest expansion based upon the highest projected precipitation and the consequence of the projected recharge rates.

5. Conclusions and recommendations

The impact of climate change on both the quantity and quality of groundwater resources in the CHLB for the next 30 years was projected using future climate conditions (AR4 and AR5 scenarios), the recharge estimation model (HELP3), and the groundwater model (SEAWAT) to create projections. Average annual temperatures and the amounts of precipitation were considered as the key indicators for the future climate conditions. In next 30 years (2045), the average annual temperature in the CHLB is projected to increase by 3.1° C under the SEACAM of AR4 and by 2.2 °C under the CanESM2 of AR5 climate conditions. The future precipitation is expected to decrease by 33.1% and 8.6% under the SEACAM and to increase by 30.5% and 6.2% under the CanESM2 in dry and wet seasons, respectively. In both future climate change scenarios, the rainfall pattern in wet season will be greatly re-distributed to receive rainfall in other months.

The impact of climate change on groundwater recharge, storage, and salinity distribution was projected. In the next 30 years, groundwater recharge is projected to increase by 17.0% and decrease by 0.7% under the CanESM2 and the SEACAM, respectively. Seasonal recharge in the wet season is projected to increase by 3.96% and decrease by 4.87% under the CanESM2 and the SEACAM, respectively. Meanwhile, aquifer storage is expected to increase for both future climate conditions, and in the future, the groundwater level is projected to continuously rise. The projected impact of future climate change on groundwater salinity and its consequent effect to the soil has been examined. The deep and shallow groundwater salinity and waterlogging have significantly increased in every scenario with almost same result until 2045. The salt-affected areas will increase by 8.08% for deep saline groundwater, by 56.92% for shallow saline groundwater, and 63.65% in the case of waterlogging. The saline groundwater areas and the waterlogged areas will expand from the flood plain of the Huai Luang River to the discharge areas. The highest expansion areas were observed under the RCP 8.5 scenario of the CanESM2 model due to the higher projected precipitation rates and as a consequence of higher projected recharge. This is due to the fact that the studied area is underlain by a relatively large and complicated dynamic basin. There are many factors of uncertainty involved in this study. By and large, in regard to the monitoring of the water level and soil salinity fluctuations, the period of study may be considered as relatively short.

In addition to groundwater salinity and waterlogging expansion, the effects of soil salinity may consequently exacerbate future livelihoods of people living in this area. Intensive preparations to control waterlogging and salinity include re-foresting areas, enhancing drainage efficiencies, improving soil textures and fertility, and introducing salt tolerant paddy rice. It is essential to implement these procedures in the CHLB.

Acknowledgements

This research study was funded by the Thailand Research Fund (TRF). The authors would like to thank Bureau 10 of the Regional Groundwater Resources in Udon Thani Province; the Department of Groundwater Resources (DGR); the Ministry of Natural Resources and Environment and the Land Development Regional Office 5 Khon Kaen; the Land Development Department (LDD); and the Ministry of Agriculture and Cooperatives for supporting the project. We are also extremely grateful to the staff of the Royal Irrigation Department (RID) and the Thai Meteorological Department (TMD) for sharing the hydrological and weather data.

References

Allan, M.J., 1994. An assessment of secondary dryland salinity in Victoria. Technical Report No.14. Centre for Land Protection Research, Department of Conservation & Natural Resources.

Arunin, S., 1984. Characteristic and Management of Salt-affected Soils in the Northeast of Thailand. Ecology and management of Problem Soil in Asia, Taiwan: Food and Fertilizer Technology Center for the Asian and Pacific Region. FFTC Book Series No. 27.

Arunin, S., 1989. Prevention of saline soil distribution by reforestation. J. Agric. Sci. 22 (2), 141–153 (in Thai).

Arunin, S., 1996. Saline Soils in Thailand. Department of Land Development, Bangkok (in Thai).

Beresford, Q., Bekle, H., Phillips, H., Mulcock, J., 2001. The Salinity Crisis: Landscapes, Communities and Politics. University of Western Australia Press, Crawley.

Casas, R.R., Pitaluga, A., 1990. Anegamiento y salinizacion de suelos en el noroeste de la Provincia de Buenos Aires. In: Bellati, J.I., Kugler, W.F., Prego, A.J., Sabella, L.J. (Eds.), Manejo de Tierras Anegadizas. Buenos Aires: Fundacion Para La Education, La Ciencia y La Cultura, pp. 259–278.

Chaowiwat, W., Danusatianpong, P., Sarinnapakorn, K., Boonya, S., 2017. Extreme Climate Prediction for Water Management Community Network under Changing Climate. The 22nd National Convention on Civil Engineering. 18–20 July 2017. Nakhon Ratchasima, Thailand.

Chatdarong, V., 2009. Past, present and future characteristics of Thai meteorological variables and impacts on water resources management. The First China-Thailand Joint Seminar on Climate Change, March 23–24. Thai Research Fund, Bangkok.

Chinvanno, S., 2014. Adaptation to Climate Change and Strategic for Developing, Projection for Building Capacity for Adaptation to Climate Change: Case Study of in Huai Luang River Basin Thailand. Southeast Asia START Regional Center (in Thai).

Chinvanno, S., Laung-Aram, V., Sangmanee, C., Thanakitmetavut, J., 2009. Future climate projection for Thailand and Mainland Southeast Asia using PRECIS and ECHAM4 climate models. Technical Report 18. Southeast Asia START Regional Center.

CHRR, 2005. Thailand Natural Disaster Profile. The Earth Institute at Columbia University Available at:. http://bit.ly/1YUvaFR.

Chylek, P., Li, J., Dubey, M.K., Wang, M., Lesins, G., 2011. Observed and model simulated 20th century Arctic temperature variability. Canadian Earth System Model CanESM2. Atmos. Chem. Phys. Discuss. https://doi.org/10.5194/acpd-11-22893-2011.

Cotanont, T., 2014. The Application of Environmental Isotopes and Fractured Analysis for Sustaninable Groundwater Development: A Case Study of Fractured Sandstone and Siltstone Aquifers, Udon Thani Province. Doctoral Dissertation. Khon Kaen University.

Deutsch, W.J., 1997. Groundwater Chemistry-fundamentals and Applications to Contamination. Lewis Publishers, New York, Boca Raton, p. 221.

DGR, 2000. Provincial Groundwater Map. Department of Groundwater Resources (in Thai).

DMR, 2009. Hydrogeological Map of Thailand 1:250,000. Department of Mineral Resources, Ministry of Natural Resources and Environment, Bangkok.

Dobermann, A., Fairhurst, T., 2000. Salinity in Rice Nutrient Disorders & Nutrient Management. Potash & Phosphate Institute of Canada and International Rice Research Institute, pp. 139–144.

DPA, 2014. Population and Homes Database of Udon Thani Province. Department of Provincial Administration, Ministry of Interior, Bangkok.

Farr, E., Henderson, W.C., 1986. Land Drainage (Longman Handbooks in Agriculture). Longman Higher Education.

Ghassemi, F., Jakeman, A.J., Nix, H.A., 1995. Salinisation of Land and Water Resources Human Causes, Extent, Management and Case Studies. 1st ed. University of New South Wales Press Ltd., Sydney, p. 526.

Green, T.R., Taniguchi, M., Kooi, H., Gurdak, J.J., Allen, D.M., Hiscock, K.M., Treidel, H., Aureli, A., 2011. Beneath the surface of global change: impacts of climate change on groundwater. J. Hydrol. 405:532–560. https://doi.org/10.1016/j.jhydrol.2011.05.002.

HAII, 2016. The Context of Climate Change in Thailand. Hydro and Agro Informatics Institute. Ministry of Science and Technology, Thailand.
Harbaugh, A.W., Banta, E.R., Hill, M.C., McDonald, M.G., 2000. MODFLOW-2000, The US Geological Survey Modular Groundwater Model-user Guide to Modularization Concepts and the Groundwater Flow Process.
IPCC, 2007. In: Solomon, S., et al. (Eds.), Climate Change 2007: the Physical Science Basis. Contribution of Working Group I to the Fourth Assessment Report of the Intergovernmental Panel on Climate Change. Cambridge University Press, Cambridge, UK, and New York, USA, p. 996.
IPCC, 2013. The physical science basic-summary for policymakers. Contribution of WGI to the Fifth Assessment Report of the Intergovernmental Panel on Climate Change.
Jarupongsakul, T., 2011. Extremely Global Warming: A Future Thailand in Crisis (in Thai).
Jyrkama, M.I., Sykes, J.F., 2007. The impact of climate change on spatially varying groundwater recharge in the grand river watershed (Ontario). J. Hydrol. 338, 237–250.
Jyrkama, M.I., Sykes, J.F., Normani, S.D., 2002. Recharge estimation for transient ground water modeling. Ground Water 40 (6), 638–648.
Kurylyk, B.L., MacQuarrie, K.T.B., 2013. The uncertainty associated with estimating future groundwater recharge: a summary of recent research and an example from a small unconfined aquifer in a northern humid-continental climate. J. Hydrol. 492: 244–253. https://doi.org/10.1016/j.jhydrol.2013.03.043.
Langevin, C.D., Thorne Jr., D.T., Dausman, A.M., Sukop, M.C., Guo, W., 2008. SEAWAT version 4: a computer program for simulation of multi-species solute and heat transport. US Geological Survey Techniques and Methods Book. 6 (chapter A22).
LDD, 2006. Saline Soil Map of Northeast Thailand Scale 1:100,000. Land Development Department, Ministry of Agriculture and Cooperatives, Bangkok.
LDD, 2013. Land Use Map of Northeast Thailand 1:100,000. Land Development Department. Ministry of Agriculture and Cooperatives, Bangkok.
Limsakul, A., Singhruck, P., 2016. Long-term trends and variability of total and extreme precipitation in Thailand. Atmos. Res. 169, 301–317.
Limsakul, A., Limjirakan, S., Sriburi, T., 2010. Observed changes in daily rainfall extremes along Thailand's coastal zone. J. Environ. Res. 32, 49–68.
Manomaiphiboon, K., Octaviani, M., Torsri, K., 2009. Regional climate modeling using RegCM3 for Thailand: past and ongoing activities. The First China-Thailand Joint Seminar on Climate Change, March 23–24. Thailand Research Fund, Bangkok.
Moeck, C., Brunner, P., Hunkeler, D., 2016. The influence of model structure on groundwater recharge rates in climate-change impact studies. Hydrogeol. J. 24:1171–1184. https://doi.org/10.1007/s10040-016-1367-1.
Naruchaikusol, S., 2016. Climate change and its impact in Thailand: a short overview on actual and potential impacts of the changing climate in Southeast Asia. TransRe Fact Sheet No. 2.
NSO, 2016. Gross Provincial Product in Thailand. National Statistical Office.
ONEP, 2016. Environmental News: The National Water Resources Committee Reported the Worst Drought Over.
Pratoomchai, W., Kazama, S., Hanasaki, N., Ekkawatpanit, C., Komori, D., 2014. A projection of groundwater resources in the Upper Chao Phraya River basin in Thailand. Hydrological Res. Lett. 8 (1):20–26. https://doi.org/10.3178/hrl.8.20.
RID, 2015. Rainfall and Steam Flow Data of Udon Thani Province. Royal Irrigation Department, Ministry of Agriculture and Cooperatives, Udon Thani Province, Thailand.
Santisirisomboon, J., 2009. Statistical downscaling of GFDL-R30 in the area of Thailand. The First China-Thailand Joint Seminar on Climate Change, March 23–24. Thailand Research Fund, Bangkok.
Saraphirom, P., Wirojanagud, W., Srisuk, K., 2013a. Impact of climate change on waterlogging and salinity distributions in Huai Khamrian subwatershed, NE Thailand. Environ. Earth Sci. J. 70:887–900. https://doi.org/10.1007/s12665-012-2178-x.
Saraphirom, P., Wirojanagud, W., Srisuk, K., 2013b. Potential impact of climate change on area affected by waterlogging and saline groundwater and ecohydrology management in northeast Thailand. Environment Asia. J. 6 (1):19–28. https://doi.org/10.14456/ea.2013.4.
Schroeder, P.R., Dozier, T.S., Zappi, P.A., McEnroe, B.M., Sjostrom, J.W., Peyton, R.L., 1994. The Hydrologic Evaluation of Landfill Performance (HELP) Model: Engineering Documentation for Version 3, EPA/600/R-94/168b. U.S. Environmental Protection Agency Office of Research and Development, Washington.
Scibek, J., Allen, D.M., 2006. Comparing modelled responses of two high-permeability unconfined aquifers to predicted climate change. Glob. Planet. Chang. 50, 50–62.
Scibek, J., Allen, D.M., Cannon, A.J., Whitfield, P.H., 2007. Groundwater–surface water interaction under scenarios of climate change using a high-resolution transient groundwater model. J. Hydrol. 333, 165–181.
SEACAM, 2014. A regional climate modelling experiment for southeast Asia: using PRECIS Regional Climate Model and selected CMIP3 Global Climate Models. The Southeast Asia Climate Analyses & Modeling.
Shrestha, S., Bach, V.T., Pandey, P.V., 2016. Climate change impacts on groundwater resources in Mekong Delta under representative concentration pathways (RCPs) scenarios. Environmental Science & Policy. J. 61, 1–13.
Srisuk, K., 1994. Genetic Characteristics of the Groundwater Regime in the Khon Kaen Drainage Basin, Northeast Thailand. Doctoral Dissertation. University of Alberta.
Srisuk, K., Nettasana, T., 2017. Climate change and groundwater resources in Thailand. Groundwater Science and Engineering J. 4 (2), 67–75.
Suwanich, P., 1986. Potash and Rock Salt in Thailand. Nonmetallic Minerals Bulletin No. 2. Economic Geology Division. Department of Mineral Resources, Bangkok.
TMD, 2015. Weather Data of Udon Thani Province. Thai Meteorological Department, Ministry of Information and Communication Technology, Bangkok.
Toews, M.W., Allen, D.M., 2009. Evaluating different GCMs for predicting spatial recharge in an irrigated arid region. J. Hydrol. 374:265–281. https://doi.org/10.1016/j.jhydrol.2009.06.022.
TRF, 2011. IPCC &TARC Report: State of Knowledge on the World and Thailand's Climate Change. T-GLOUB, Thailand Research Fund (in Thai).
van Vuuren, D., Edmonds, J., Kainuma, M., Riahi, K., Thomson, A., Hibbard, K., 2011. The representative concentration pathways: an overview. Clim. Chang. 109:5–31. https://doi.org/10.1007/s10584-011-0148-z.
Weiss, J., 2009. The Economics of Climate Change in Southeast Asia: A Regional Review. © Asian Development Bank http://hdl.handle.net/11540/179 (License: CC BY 3.0 IGO).
Wichaidit, P., 1997. The Manual of Northeastern Thailand Saline Map. Department of Land Development, Bangkok, pp. 174–176.
World Bank, 2011. The World Bank Supports Thailand's Post-floods Recovery Effort.
Yusuf, A.A., Francisco, H.A., 2009. Climate Change Vulnerability Mapping for Southeast Asia, Singapore: Economy and Environment Program for Southeast Asia (EEPSEA).
Yuvaniyama, A., 2004. Manual of Saline Soils Management and Reclamation, Technical Paper of Research and Development of Salt-affected Areas Group. Land Development Department, Bangkok (in Thai).
Zektser, I.S., Loaiciga, H.A., 1993. Groundwater fluxes in global hydrologic cycle: past, present, and future. J. Hydrol. 144, 405–427.
Zheng, C., Wang, P.P., 1999. MT3DMS: A Modular three Dimensional Multispecies Transport Model for Simulation of Advection, Dispersion, and Chemical Reactions of Contaminants in Groundwater Systems. US Army Engineer Research and Development Center, Vicksburg, MS.